© 2017. Published by The Company of Biologists Ltd | Journal of Experimental Biology (2017) 220, 2452-2475 doi:10.1242/jeb.156646

RESEARCH ARTICLE

The Ol$_1$mpiad: concordance of behavioural faculties of stage 1 and stage 3 *Drosophila* larvae

Maria J. Almeida-Carvalho[1], Dimitri Berh[2,3], Andreas Braun[4,5], Yi-chun Chen[6,*], Katharina Eichler[7], Claire Eschbach[7], Pauline M. J. Fritsch[8], Bertram Gerber[6,9,10,*], Nina Hoyer[11], Xiaoyi Jiang[3], Jörg Kleber[6], Christian Klämbt[2], Christian König[12,13], Matthieu Louis[4,5,14], Birgit Michels[6], Anton Miroschnikow[15], Christen Mirth[1,16], Daisuke Miura[17], Thomas Niewalda[6,*], Nils Otto[2], Emmanouil Paisios[6], Michael J. Pankratz[15], Meike Petersen[11], Noel Ramsperger[18], Nadine Randel[7], Benjamin Risse[2,3], Timo Saumweber[6], Philipp Schlegel[15], Michael Schleyer[6], Peter Soba[11], Simon G. Sprecher[8], Teiichi Tanimura[17], Andreas S. Thum[18], Naoko Toshima[6,17], Jim W. Truman[7,19], Ayse Yarali[10,12] and Marta Zlatic[7]

ABSTRACT

Mapping brain function to brain structure is a fundamental task for neuroscience. For such an endeavour, the *Drosophila* larva is simple enough to be tractable, yet complex enough to be interesting. It features about 10,000 neurons and is capable of various taxes, kineses and Pavlovian conditioning. All its neurons are currently being mapped into a light-microscopical atlas, and Gal4 strains are being generated to experimentally access neurons one at a time. In addition, an electron microscopic reconstruction of its nervous system seems within reach. Notably, this electron microscope-based connectome is being drafted for a stage 1 larva – because stage 1 larvae are much smaller than stage 3 larvae. However, most behaviour analyses have been performed for stage 3 larvae because their larger size makes them easier to handle and observe. It is therefore warranted to either redo the electron microscopic reconstruction for a stage 3 larva or to survey the behavioural faculties of stage 1 larvae. We provide the latter. In a community-based approach we called the Ol$_1$mpiad, we probed stage 1 *Drosophila* larvae for free locomotion, feeding, responsiveness to substrate vibration, gentle and nociceptive touch, burrowing, olfactory preference and thermotaxis, light avoidance, gustatory choice of various tastants plus odour–taste associative learning, as well as light/dark–electric shock associative learning. Quantitatively, stage 1 larvae show lower scores in most tasks, arguably because of their smaller size and lower speed. Qualitatively, however, stage 1 larvae perform strikingly similar to stage 3 larvae in almost all cases. These results bolster confidence in mapping brain structure and behaviour across developmental stages.

KEY WORDS: Sensory processing, Locomotion, Feeding, Learning and memory, Navigation

INTRODUCTION

Mapping brain function to brain structure is a fundamental task for neuroscience. Focusing on behaviour as the integrated function of the brain, we describe here the behavioural faculties of stage 1 *Drosophila* larvae. This provides a resource for relating behavioural function to the upcoming description of their connectome (e.g. Ohyama et al., 2015; Berck et al., 2016; Fushiki et al., 2016; Jovanic et al., 2016; Schlegel et al., 2016; Schneider-Mizell et al., 2016; Zwart et al., 2016; Eichler et al., 2017).

Drosophila is known as a genetic model system. It allows study of the principles of heredity, development and brain function. The uncovered genetic and molecular networks are highly conserved, examples including early embryonic development, ion channel and synaptic function (e.g. Johnston and Nüsslein-Volhard, 1992; Littleton and Ganetzky, 2000). This genetic and molecular similarity defines *Drosophila* as a model for biomedical science.

In the 1970s, behavioural genetics of *Drosophila* gained momentum. Early study cases explored phototaxis (Benzer, 1967), circadian behaviour (Konopka and Benzer, 1971) and Pavlovian learning (Dudai et al., 1976; Heisenberg et al., 1985; Tully and Quinn, 1985). The range of experimentally accessible behaviours now includes various further olfactory and gustatory behaviours, courtship, feeding and aggressive behaviours as well as operant and other learning paradigms (Zhang et al., 2010, and references therein). These studies received a boost by their combination with new methods for transgenesis and transgene expression (Rubin and Spradling, 1982; O'Kane and Gehring, 1987; Brand and Perrimon, 1993). These and related techniques now allow the comparatively convenient expression of transgenes, in any cell or group of cells, at any time (e.g. Venken et al., 2011). Thus, *Drosophila* is a powerful model system to understand not 'only' molecular and cellular processes but also their function in behaviourally meaningful circuitry (e.g. Sivanantharajah and

[1]Gulbenkian Institute of Science, 2780-156 Oeiras, Portugal. [2]Institute of Neurobiology and Behavioural Biology, University of Münster, 48149 Münster, Germany. [3]Department of Mathematics and Computer Science, University of Münster, 48149 Münster, Germany. [4]EMBL/CRG Systems Biology Unit, Centre for Genomic Regulation, 08003 Barcelona, Spain. [5]Universitat Pompeu Fabra, 08002 Barcelona, Spain. [6]Leibniz Institute for Neurobiology (Genetics), 39118 Magdeburg, Germany. [7]Janelia Research Campus, Howard Hughes Medical Institute, Ashburn, VA 20147, USA. [8]Department of Biology, University of Fribourg, 1700 Fribourg, Switzerland. [9]Institute of Biology, Otto von Guericke University Magdeburg, 39118 Magdeburg, Germany. [10]Center for Behavioral Brain Sciences, Otto von Guericke University Magdeburg, 39106 Magdeburg, Germany. [11]Center for Molecular Neurobiology, University of Hamburg, 20251 Hamburg, Germany. [12]Leibniz Institute for Neurobiology (Molecular Systems Biology), 39118 Magdeburg, Germany. [13]Institute of Pharmacology and Toxicology, Otto von Guericke University Magdeburg, 39118 Magdeburg, Germany. [14]Department of Molecular, Cellular, and Developmental Biology, University of California, Santa Barbara, CA 93117, USA. [15]LIMES-Institute, University of Bonn, 53115 Bonn, Germany. [16]School of Biological Sciences, Monash University, Melbourne, VIC 3800, Australia. [17]Department of Biology, Kyushu University, 819-0395 Fukuoka, Japan. [18]Department of Biology, University of Konstanz, 78464 Konstanz, Germany. [19]Friday Harbor Laboratories, University of Washington, Friday Harbor, WA 98250, USA.
Authors are presented in alphabetical order.

*Authors for correspondence (bertram.gerber@lin-magdeburg.de; thomas.niewalda@lin-magdeburg.de; yi-chun.chen@lin-magdeburg.de)

B.G., 0000-0003-3003-0051

Received 17 January 2017; Accepted 3 May 2017

Journal of Experimental Biology

Journal of Experimental Biology (2017) 220, 2452-2475 doi:10.1242/jeb.156646

Zhang, 2015) – as envisaged by Hotta and Benzer (1970). The elegance of the uncovered minimal biological circuits defines the inspiration of *Drosophila* for engineering, informatics and robotics (e.g. Frye and Dickinson, 2004).

With a slight delay, larval *Drosophila* entered the stage as subjects of behavioural neurogenetics (e.g. Aceves-Piña and Quinn, 1979; Rodrigues, 1980; Heisenberg et al., 1985), with revived interest since the 1990s (Stocker, 1994; Cobb, 1999; Sokolowski, 2001; Gerber and Stocker, 2007; Gomez-Marin and Louis, 2012; Keene and Sprecher, 2012; Diegelmann et al., 2013). Larvae possess 10 times fewer neurons than adult flies, but feature fundamental adult-like circuit motifs (for example, in the olfactory pathways: Vosshall and Stocker, 2007; Stocker, 2008) as well as fundamental faculties of behaviour – with the obvious exception of reproductive behaviours and flight. Beyond locomotion and feeding, these faculties include various forms of taxes, kineses and Pavlovian learning. Thus, the larva offers a fortunate balance of being simple enough to be tractable, yet complex enough to be interesting. Indeed, in the foreseeable future, the larva's 10,000-neuron nervous system will be mapped into a light-microscopical cell-by-cell atlas (Li et al., 2014), and Gal4 strains can be generated to experimentally access these neurons one at a time. In addition, an electron microscopic reconstruction of the full larval brain and ventral nerve cord, at synaptic resolution, seems within reach (e.g. Ohyama et al., 2015; Berck et al., 2016; Fushiki et al., 2016; Jovanic et al., 2016; Schneider-Mizell et al., 2016; Zwart et al., 2016; Eichler et al., 2017). These resources will allow the mapping of behaviour onto circuitry with an unprecedented combination of ease, completeness and precision.

Notably, the electron microscope-based connectome is being drafted for a stage 1 larva – because they are considerably smaller than stage 3 larvae and thus are quicker to image using electron microscope techniques. However, the vast majority of published behaviour analyses have been performed for stage 3 larvae – as their larger size makes them easier to handle. Although light microscopical observations have not yet ascertained major qualitative discrepancies in the neuroanatomy between stage 1 and stage 3 larvae, it is not trivial to show the utility of the stage 1 connectome for guiding behavioural analyses in stage 3 larvae. This is because not only growth but also neurogenesis continues across larval stages in at least some brain regions (Ito and Hotta, 1992). To bolster confidence in connectome–behaviour mappings, it is thus warranted to either redo the electron microscopic reconstruction for a stage 3 larva or survey the behavioural faculties of stage 1 larvae. We provide the latter.

MATERIALS AND METHODS

The aim of this study was to test stage 1 *Drosophila* larvae (L1) for their behavioural faculties, with a focus on assays that have been routinely used for stage 3 larvae (L3). When designing the present experiments, three general considerations were borne in mind. Firstly, we wanted to employ methods of experimentation, data acquisition and analysis as similar as possible to those previously used for L3. These methods differ to some extent across assays and laboratories. Secondly, and conflictingly, we aimed at homogeneity of methods across the assays of this survey in order to allow meaningful comparisons across assays. Thirdly, in some cases it did not seem reasonable to use the very same experimental parameters for L1 and L3. For example, using the same parameters for nociceptive stimulation as in L3 would have been damaging if not lethal for L1. The work described below thus corresponds to the reasoned judgement of the contributing scientists as to what is a reasonable balance of these considerations.

We first present general aspects of our methods regarding the larvae and statistics used. We then present counting-based assays, followed by assays based on video tracking.

Larvae

We used L1 from the Canton-S wild-type strain, aged 30 h (±2 h) after egg laying. Three days before the experiment, approximately 350 adult flies were transferred to apple juice agar plates (25% juice and 1.25% sucrose in 2.5% agar solution), and maintained at 25°C, 60–70% relative humidity and a 12 h:12 h light:dark cycle. One day before each experiment, flies were allowed to lay eggs for 2 h on a fresh apple juice agar plate, and then removed. After 30 h, we collected approximately 30 larvae from the apple juice agar plates, briefly rinsed them in a droplet of water and started the experiment. In cases when L3 were also used, these were aged 5 days (120 h) after egg laying. Exceptions to the above are mentioned in the description of the behavioural paradigms.

Statistics

Non-parametric statistics were applied throughout. For comparisons to chance levels (i.e. to zero), one-sample sign tests (OSS) were used (R 3.4.0; R Core Team, 2017). For between-group comparisons, Kruskal–Wallis tests (KW) and Mann–Whitney *U*-tests (MWU) were employed as appropriate (Statistica 12, StatSoft). We used a Bonferroni correction whenever warranted to maintain an error rate below 5%. Data are displayed as box plots, where the middle line shows the median, the box boundaries are the 25% and 75% quantiles, and the whiskers the 10% and 90% quantiles. Exceptions to the above are mentioned in the respective figure legends.

Behavioural paradigms

Olfactory preference

We used Petri dishes of 55 mm inner diameter (Sarstedt, Nümbrecht, Germany), filled with freshly boiled 1% agarose solution. Once the agarose had solidified, dishes were stored until use at 4°C for up to a week.

We added 10 µl of *n*-amyl acetate (AM, CAS: 628-63-7; Merck, Darmstadt, Germany; diluted 1:50 in paraffin oil, CAS: 8012-95-1; Merck) into Teflon containers of 5 mm diameter. These containers were then closed by a lid perforated with 5–10 holes, each of approximately 0.5 mm diameter and placed at the edge of the dish. The position of the container was varied (left, right, front, back) to average-out spurious effects of the experimental surround. Paraffin oil is without apparent behavioural significance as an odour (Saumweber et al., 2011).

We placed 30 larvae in the middle of each Petri dish and closed the lid. At the time point(s) given in Results, we scored the number of larvae located on the AM side, on the other side, or on a 10 mm-wide 'neutral' middle strip. We calculated an olfactory preference index ($\mathrm{Pref}_{\mathrm{Olfactory}}$) as the difference between the number of larvae on the AM side (n_{AM}) minus the number of larvae on the other side (n_{other}) and divided this difference by the total number (n_{total}) of larvae on the dish:

$$\mathrm{Pref}_{\mathrm{Olfactory}} = (n_{\mathrm{AM}} - n_{\mathrm{other}})/n_{\mathrm{total}}. \quad (1)$$

Thus, $\mathrm{Pref}_{\mathrm{Olfactory}}$ values were constrained between 1 and −1; positive values indicate preference for AM and negative values indicate aversion to AM.

In a second set of experiments, 1-octanol (OCT, CAS: 111-87-5; Merck) was used as the odour.

Gustatory preference

We prepared Petri dishes of 55 mm inner diameter (Sarstedt, Nümbrecht, Germany) such that one side was filled with 1% agarose solution that in addition contained, for example, 2 mol l^{-1} fructose (CAS: 57-48-7, purity 99%; Sigma-Aldrich, Steinheim, Germany) while the other side was filled with 1% agarose only ('pure'). After preparation, Petri dishes were covered with their lids and left at room temperature until the experiment started later the same day.

The position of the tastant side was varied (left, right) to average-out spurious effects of the experimental surround. We placed approximately 30 (L1) or 15 (L3) larvae in the middle of these Petri dishes and closed the lid. At the time points given in Results, we scored the number of larvae located on the pure side, the fructose side or a 5 mm-wide 'neutral' middle strip. We calculated a gustatory preference index ($Pref_{Gustatory}$) as the number of larvae on the fructose side (n_{Fru}) minus the number of larvae on the pure side (n_{pure}) and divided this difference by the total number of larvae on the dish:

$$Pref_{Gustatory} = (n_{Fru} - n_{pure})/n_{total}. \quad (2)$$

Thus, $Pref_{Gustatory}$ values were constrained between 1 and −1; positive values indicate preference for fructose and negative values indicate aversion to fructose.

In addition, experiments were performed as above for fructose, but with 2 mol l^{-1} arabinose (CAS: 10323-20-3, purity 99%; Sigma-Aldrich), 2 mol l^{-1} sorbitol (CAS: 50-70-4, purity 98%; Sigma-Aldrich), 5 mmol l^{-1} quinine hemisulfate (CAS: 6119-70-6, purity 92%; Sigma-Aldrich), 10 mmol l^{-1} aspartic acid (CAS: 56-84-8, purity ≥99%; Sigma-Aldrich) or NaCl (CAS: 7647-14-5, purity ≥99.5%; Roth, Karlsruhe, Germany; at the concentrations mentioned in Results).

Odour–tastant associative learning: fructose and aspartic acid

We followed standard methods for a two-odour, reciprocal conditioning paradigm (Scherer et al., 2003; Neuser et al., 2005; for detailed protocols, see Gerber et al., 2010, 2013; Apostolopoulou et al., 2013; Michels et al., 2017). To take into account the small size of L1, we used smaller Petri dishes (55 mm diameter) than is standard for L3 (90 mm), filled with either only 1% agarose ('pure') or 1% agarose plus 2 mol l^{-1} fructose as a reward. Olfactory choice performance of larvae was compared after either of two reciprocal training regimens: one set of larvae received *n*-amyl acetate (AM; CAS: 628-63-7; Merck; diluted 1:50 in paraffin oil) together with fructose as a reward (+) and 1-octanol (OCT; CAS: 111-87-5; Sigma-Aldrich; undiluted) without reward (AM+/OCT; this cycle of 5 min/5 min training trials was performed for a total of 3 times); the other set of larvae underwent reciprocal training (AM/OCT+). The sequence of training trials was balanced across repetitions of the experiment (i.e. OCT/AM+ and in the reciprocal case OCT+/AM). Then, animals were tested for their relative preference between AM versus OCT. They were placed to the middle of a Petri dish equipped with AM on one side and OCT on the other. After 3 min, their numbers were scored as on the AM side (n_{AM}), the OCT side (n_{OCT}) or in the middle, and preference scores were calculated as:

$$Pref = (n_{AM} - n_{OCT})/n_{total}. \quad (3)$$

Appetitive associative memory is indicated by a relatively higher preference for AM after AM+/OCT training compared with the reciprocal AM/OCT+ training. These differences in preference were quantified by the associative performance index (PI):

$$PI = (Pref_{AM+/OCT} - Pref_{AM/OCT+})/2. \quad (4)$$

Thus, positive PI values indicate appetitive memory and a rewarding effect of the tastant, while negative PI values indicate aversive memory and a punishing effect of the tastant.

In L3, it was shown that the preference for the previously rewarded odour is a form of learned search behaviour, such that the location of the odour source during the test informs the animal about the likely location of the reward. Fittingly, such learned search is abolished if the test is performed in the presence of the sought-for reward (Gerber and Hendel, 2006; Saumweber et al., 2011; Schleyer et al., 2011, 2015a,b; see also Schleyer et al., 2013). To determine whether the same organization of behaviour is found in L1, we ran the test after the above training regimen either in the absence or in the presence of fructose throughout the test Petri dish.

The same type of behavioural paradigm was used for 10 mmol l^{-1} aspartic acid (CAS: 56-84-8, purity ≥99%; Sigma-Aldrich) as a reinforcer.

Odour–tastant associative learning: quinine and salt

The behavioural paradigm followed the methods described above for odour–fructose and odour–aspartic acid learning, except that 5 mmol l^{-1} quinine (CAS: 6119-70-6; Sigma-Aldrich) was used as a reinforcer. Notably, in L3, it was shown that 5 mmol l^{-1} quinine is an effective punishment. In particular, the preference for the previously non-punished odour is a form of escape behaviour that is expressed only when the testing situation warrants escape, i.e. if the quinine punishment is present during the test (Gerber and Hendel, 2006; Schleyer et al., 2011, 2015a; El-Keredy et al., 2012; see also Schleyer et al., 2013). To see whether the same organization of behaviour is found in L1, we ran the test after the above training regimen either in the absence or in the presence of quinine throughout the test Petri dish.

The same type of behavioural paradigm was used for salt (0.2 mol l^{-1} NaCl) as reinforcer. Of note, in L3, it was shown that low concentrations of salt can be rewarding, while high concentrations of salt can be punishing. Specifically, based on the literature concerning L3, 0.2 mol l^{-1} NaCl is expected to be an effective reward, and learned search would be abolished if the test is performed in the presence of that reward (Gerber and Hendel, 2006; Niewalda et al., 2008; Russell et al., 2011; see also Schleyer et al., 2013). To see whether this is the case in L1 too, we ran the test after the above training regimen either in the absence or in the presence of salt throughout the test Petri dish. As our results indicated that, unexpectedly, 0.2 mol l^{-1} NaCl is a punishment to L1, we repeated the experiment for L3 as well; Petri dishes of the same size as for L1 were used for these experiments.

Odour–DAN activation associative learning

Odour–dopaminergic neuron (DAN) activation associative learning experiments were performed according to Rohwedder et al. (2016), with the modifications described in Eichler et al. (2017).

Double heterozygous L1 of the experimental genotype express Chrimson as effector in DANs innervating the mushroom body medial lobe. These larvae were the offspring of a cross of P{GMR58E02-GAL4}attP2 (henceforth abbreviated as R58E02-Gal4; Liu et al., 2012; Bloomington Stock Center no. 41347) and P{20XUAS-IVS-CsChrimson.mVenus}attP18 (henceforth abbreviated as UAS-Chrimson; Klapoetke et al., 2014; Bloomington Stock Center no. 55134). Effector control larvae resulted from a cross of UAS-Chrimson and a strain carrying an empty attP2 landing site (Pfeiffer et al., 2008; Jenett et al., 2012). Driver control larvae resulted from a cross of R58E02-Gal4 and a strain carrying an empty attP18 landing site (Pfeiffer et al., 2010).

Journal of Experimental Biology (2017) 220, 2452-2475 doi:10.1242/jeb.156646

Eggs were incubated at 25°C in constant darkness on 4% agarose with a yeast and water paste including retinal at 0.5 mmol l^{-1} final concentration. At 40 h after egg laying, groups of 30 individual L1 were placed on plates filled with 4% agarose. The odour ethyl acetate (EA, CAS: 141-78-6; Sigma-Aldrich; diluted 100 times in distilled water) was presented on filter papers located on the lid. In this situation, the larvae were exposed to constant red light from above (626 nm, 3.5 µW mm^{-2}; represented by an asterisk, *) for 3 min. Subsequent to this EA*-trial, larvae were transferred to a new plate, and were left for 3 min without odour and in darkness (blank). This paired EA*/blank training cycle was repeated two more times. A second set of larvae underwent reciprocal training with unpaired presentations of odour and red light (EA/*). The sequence of training trials was balanced across repetitions of the experiment (i.e. blank/EA* and in the reciprocal case */EA). Then, animals were tested for their relative preference for EA versus blank. They were placed to the middle of a Petri dish of 90 mm inner diameter equipped with EA on one side and a blank filter paper on the other. After 5 min, their numbers were scored as on the EA side (n_{EA}), the blank side (n_{blank}) or in a 10 mm middle strip, and preference scores were calculated as:

$$\text{Pref} = (n_{EA} - n_{blank})/n_{total}. \quad (5)$$

Appetitive associative memory is indicated by a relatively higher preference for EA after EA*/blank training compared with the reciprocal EA/* training. These differences in preference were quantified by the associative PI:

$$\text{PI} = (\text{Pref}_{EA*/blank} - \text{Pref}_{EA/*})/2. \quad (6)$$

Light/dark–electric shock associative learning

The behavioural paradigm follows von Essen et al. (2011), modified into a two-group paradigm. To take into account the small size of L1, we used 55 mm Petri dishes throughout (Greiner Bio-One, Wemmel, Belgium) filled with 1% agarose (CAS: 3810.4; Roth). Petri dishes were equipped with two copper electrodes located on opposing sides of the Petri dish, through which a 100 V shock could be applied (Müter RTT3, 0-270 V AC, 2.5 A, 675 W). For light stimulation, LEDs (Osram LED, 80012 White) were used at an intensity of 760 lx.

A cohort of larvae was transferred onto a Petri dish and the light was switched on for 1 min (~45 animals for L1 and ~25 animals for L3 per cohort; this ensured that for both L1 and L3, about 20 animals remained for scoring during the test). During the last 30 s of this light stimulation, the larvae were exposed to a continuous electric shock (+). Afterwards, the light was switched off and the larvae were left untreated for 5 min (light+/dark training). This training cycle was repeated 4 more times (total duration of light exposure: 5×1 min=5 min). A second group of larvae underwent light/dark+ training (total duration of light exposure: 5×5 min=25 min). The sequence of training trials was balanced across repetitions of the experiment (i.e. either as above, or dark/light+ and dark+/light). Then, the larvae were tested for their preference between light and dark on a test Petri dish equipped with a modified lid such that two quarters were covered by black tape. Larvae were placed in the centre of the test Petri dish and after 5 min their numbers were scored according to their location on a light (n_{light}) or dark (n_{dark}) quadrant:

$$\text{Pref} = (n_{light} - n_{dark})/n_{total}. \quad (7)$$

Memory is indicated by stronger light avoidance after light+/dark training than after dark+/light training. This difference in preference was quantified by the PI:

$$\text{PI} = (\text{Pref}_{light+/dark} - \text{Pref}_{dark+/light})/2. \quad (8)$$

As mentioned above, the total duration of light exposure was not equal between groups (5 min versus 25 min). Therefore, in order to test whether such differences in light exposure can in themselves lead to differences in light preference, a control experiment was run (for L3); it featured training-like handling and light exposure for both groups, but omitted electric shocks.

Food intake

Larvae were raised and staged as described above except that a droplet of yeast paste was added to the apple juice agar plates used for egg laying. Also, the L3 used were younger than indicated above, i.e. 96±1 h after egg laying. L3 were transferred from agar plates to vials containing standard fly food 48 h after egg laying.

Larvae were washed and transferred onto apple juice agar plates (L1: 30–40 larvae/plate; L3: 5 larvae/plate); these plates contained 0.1 g fluorescent yeast paste (0.3% fluorescein sodium salt, Sigma-Aldrich, F6377). Larvae were then left untreated for 5, 10, 20 or 30 min. All experiments were performed at 18°C. Afterwards, larvae were removed, washed and transferred onto an adhesive tape wrapped around a glass slide to incapacitate them. For image acquisition, a fluorescence binocular (Olympus SZX 12) with mounted camera (F-View U-Tv1 with CellF 2.8 software, both Olympus) was used. ImageJ was used to calculate fluorescence intensity F of the whole larva by averaging overall pixel values for each individual larva. Fluorescence intensity data of individual larvae from the 10, 20 and 30 min time points were separately normalized to the mean F of all individuals at the 5 min time point for L1 and L3 data, respectively. Such separate normalization for L1 and L3 larvae is warranted because the size difference between them makes it necessary to adjust image acquisition (zoom) accordingly.

Incapacitating the larvae prior to image acquisition by exposure to high (~60°C) or low (<−20°C) temperature turned the larvae opaque, resulting in an impractically diffuse, low-contrast fluorescence signal. Additionally, using yeast coloured with crimson red powder, an assay that we previously used for L3 (Schoofs et al., 2014), proved to be impractical in L1 as the staining in the gut was too weak (not shown).

Burrowing

For the burrowing assay, 10 larvae (either L1 or L3) were collected and placed onto the surface of a 60 mm-diameter tissue culture dish filled with yeast diet (180 g l^{-1} yeast, Lesaffre SAF-Instant Red nos 15909, 31105 and 31150, in 0.5% agar). Larvae were left to forage and the percentage of larvae remaining on the surface of the food was determined at 0, 5, 15, 30 and 60 min.

Mechano-nociception

Strains of *Drosophila*, rearing conditions and staging procedures were as described above except that egg laying was allowed for 2 h on 60 mm grape juice agar dishes at 25°C, 70% relative humidity and a 12 h:12 h light:dark cycle. L3 were staged and grown on yeast paste containing grape juice agar plates and assayed at 96±2 h after egg laying.

Mechano-nociception assays were performed as described in Hwang et al. (2007) with some modifications. L1 or L3 were placed on a 100 mm, 2% agar dish overlaid with 1 ml of distilled water to create a thin water film on the agar surface. Straight-moving larvae

Journal of Experimental Biology (2017) 220, 2452-2475 doi:10.1242/jeb.156646

were stimulated with a von Frey filament. In order to be noxious without actually lesioning the larvae, stimulation was calibrated to exert a force of 20 mN for L1 and 50 mN for L3. Stimulation consisted of briefly (∼1 s) exerting the respective force to the dorso-lateral side of a mid-abdominal larval segment. Each larva was stimulated twice within 2 s. Only the response to the second stimulation was scored according to Hwang et al. (2007) as: no response, stop, stop and turn, or rolling (360 deg rotation along the body axis); in addition, bending was introduced to score for an incomplete nociceptive response (simultaneous convulsive head and tail movements) that did not result in rolling. In order to compare proportions of larvae displaying each type of behaviour at L1 versus L3 stages, we used two-tailed *Z*-tests.

Touch

Strains of *Drosophila*, rearing conditions and staging procedures were as described in the previous section. Larvae were briefly (approximately 1 s) and gently brushed with an eyelash on the T2 segment, which was identified by the presence of spiracles. Each larva was touched four times and the behaviour was scored according to Kernan et al. (1994) as: no response, stop, head withdrawal and turn, backward wave and turn, backward crawl and turn. In order to compare proportions of larvae displaying each type of behaviour at L1 versus L3 stages, we used two-tailed *Z*-tests.

Rolling in response to optogenetic activation of basin interneurons

Experiments on rolling upon basin interneuron activation were performed using the experimental set-up described by Ohyama et al. (2013) and following the methods of Ohyama et al. (2015), with modifications described below.

Double heterozygous L1 of the experimental genotype express Chrimson as effector in basin interneurons. They were the offspring from the cross of male w[1118];P{GMR72F11-Gal4}attP2 (henceforth abbreviated as R72F11-Gal4; Ohyama et al., 2015; Bloomington Stock Center no. 39786) and female UAS-Chrimson (Klapoetke et al., 2014; Bloomington Stock Center no. 55134), and were tested for rolling behaviour upon light stimulation. To obtain effector control larvae, female UAS-Chrimson flies were crossed to males of a strain carrying an empty attP2 landing site (Pfeiffer et al., 2008; Jenett et al., 2012) and assayed for rolling behaviour; R72F11-Gal4 larvae were used as the driver control.

Eggs were incubated at 25°C in constant darkness on standard fly food with retinal at 0.5 mmol l^{-1} final concentration. For control experiments without retinal, larvae of the experimental genotype were grown on retinal-free food. At 24–30 h after egg laying, individual L1 were collected with 15% sucrose and individually placed on a 4% agar plate for video tracking as described in Ohyama et al. (2013); the illumination required for tracking was provided by an infrared light array (850 nm). After a 30 s accommodation period, a red light stimulus (627 nm, 160 µW mm^{-2}) was applied for 15 s. This 30 s/15 s cycle was repeated 4 more times. If a larva could not be tracked for technical reasons during at least four of the stimulations of this protocol, its data were discarded (this happened in <10% of the cases when image contrast was insufficient). From the tracked images, rolling behaviour was scored according to Tracey et al. (2003). A larva was classified as 'rolling' if it showed rolling behaviour (Movie 1) at least once during the stimulation protocol.

Video tracking of the response to 'buzz' mechanosensory disturbance

To measure the locomotor changes by mechanosensory disturbance, we used the 'buzz' set-up described in Eschbach et al. (2011) and Saumweber et al. (2014), with minor changes to accommodate the small size of L1. Specifically, (i) a higher-resolution camera (Basler ace acA2040-90umNIR, Ahrensburg, Germany), (ii) new, custom-written software, and (iii) agarose-filled Petri dishes of smaller diameter (90 mm) were used. In brief, either L1 or L3 were tracked in groups of about 20 with 10 such groups being assayed. After an accommodation period of 4.8 s, a single mechanosensory disturbance was delivered by a loudspeaker below the Petri dish (duration: 0.2 s, frequency: 100 Hz, defined as 'buzz'). Following Eschbach et al. (2011), the baseline translational run speed and the baseline angular speed were determined for the 2 s before the buzz, for each individual larva. Data from these individual larvae during the 4 s after buzz onset were then expressed as relative translational run speed and relative angular speed, normalized to their individual baseline, in 1 s bins. Negative scores thus indicate slowing down and turning less, respectively, while positive scores indicate speeding up and turning more.

Video tracking of 'free' locomotion

Larvae were staged and maintained as described above, except that neither sugar nor juice was added to the yeast agar plate (5% agar, food grade, CAS: 9002-18-0; Applichem, Darmstadt, Germany; with 0.125% acetic acid, Sigma-Aldrich).

Tracking experiments were performed according to Risse et al. (2013, 2014). In brief, cohorts of 18–22 L1 were placed on a 55 mm×55 mm test arena covered with 0.8% agar (food grade, CAS: 9002-18-0; Applichem). Upon placement onto this test arena, the larvae were allowed a ∼2 min period to acclimate until a 5 min window for data acquisition started, at 10 frames s^{-1} (Movie 2, top; Movie 3). The minimum track length analysed was 600 frames (1 min). A total of 16 larval cohorts yielded 294 tracks with a median track length of 1199 frames (∼2 min).

Locomotion of L1 was compared with that of L3 (Movie 2, bottom; Movie 3). L3 are about 4 times larger than L1 (median body length: L1 1.29 mm, L3 5.10 mm; based on >300 larvae each). To obtain the same resolution in the recordings as for L1 (40 pixels per larval length), L3 were filmed on a larger (225 mm×225 mm) test arena. Also, as L3 are quicker in overcoming their initial disorientation upon placement onto the test arena, the 5 min data acquisition window started after a ∼1 min accommodation period for L3. From 16 larval cohorts, this yielded 370 tracks with a minimum track length of 600 frames (median: 1334 frames, ∼2 min 13 s). These tracks were analysed using FIMTrack (fim.uni-muenster.de) and according to Otto et al. (2016) were classified into 'go' and 'reorientation' phases; data during collisions were not analysed.

From the gathered tracks, the following parameters were determined (see Risse et al., 2013, 2014, for details): (i) frequency of peristaltic contractions during go-phases (based on the temporal distribution of body size); (ii) absolute speed during go-phases, and speed relative to larval length; (iii) probability distribution of bending angles across all recorded frames and larvae; (iv) turn rate (based on those transitions between go and reorientation phases that entailed a change in bearing of at least 30 deg); (v) distance gained from the origin, relative to larval length.

Video tracking of thermotaxis

Larvae were staged and maintained as described in the preceding section. Measurements of thermotaxis follow Risse et al. (2014). In brief, a temperature gradient was established ranging from 38°C to 14°C in a 225 mm×225 mm tracking area, with a linear range from 33°C to 18°C at a gradient of 0.08°C mm^{-1}. Reflecting the

Journal of Experimental Biology (2017) 220, 2452-2475 doi:10.1242/jeb.156646

differences in absolute size and exploration range (see Results), the observation area for L3 was a 190 mm×190 mm area within this linear range. For L1, the observation area was 55 mm×55 mm, spanning a 33–29°C temperature range, temperatures that are aversive for L1 and L3 (Garrity et al., 2010).

Groups of 15–20 L1 or L3 were placed along the 33°C isothermal line. L1 were allowed ∼2 min to accommodate themselves until a 4 min 40 s window for data acquisition started, at 10 frames s^{-1}. The minimum track length analysed was 600 frames (1 min). A total of 15 cohorts of L1 yielded 362 such tracks with a median track length of 1398 frames (∼2 min 20 s).

Given that L3 are quicker than L1 in overcoming their initial disorientation upon placement in the tracking area, L3 were allowed only a 1 min accommodation period before data acquisition started. This yielded 336 tracks of >600 frames with a median track length of 1382 frames (∼2 min 18 s).

Tracks were analysed using FIMTrack (fim.uni-muenster.de) and according to Otto et al. (2016) were classified into 'go' and 'reorientation' phases; data during collisions were not analysed. From the gathered tracks the following parameters were determined: (i) median distance to the cold side of the observation area over time, with the origin of the respective track defined as 100% distance; for L1, the cold side corresponds to the 29°C isothermal line; for L3, it corresponds to the 18°C isothermal line; (ii) bearing angle to the cold side during go-phases, taking the median of all frames of a given larva; a bearing angle of 0 deg implies larvae are headed straight towards the cold side; a bearing angle of 180 deg implies they are headed straight to the hot side; (iii) absolute speed, and speed relative to larval length, during go-phases; (iv) probability distribution of bending angles across all observed larvae; (v) turn rate, based on those transitions between go-/reorientation-/go-phases that entailed a change in bearing between the go-phases of at least 30 deg; (vi) distance gained from the origin of the track, relative to larval length.

Video tracking of light avoidance

Larvae were staged and maintained as described in the preceding section. The analysis of light avoidance followed Kane et al. (2013) and Risse et al. (2014). In brief, a dark–light boundary was established using an LCD projector with a programmed light pattern. We projected an annulus of light (1450 lx) onto a dark agar surface (80 lx). Dimensions were adjusted to the body size of L1 and L3 (L1: radius of the inner dark area r_{dark}=7.5 mm, width of light annulus w=2.5 mm; L3: r_{dark}=42.5 mm, w=5.5 mm).

We placed 15–20 larvae in the middle of the dark area and allowed them to move for 7 min. The location of the larvae was determined as the location of their centroid. To assess the probability of avoidance behaviour when the larvae encounter light, we identified animals that entered the dark–light border zone and then determined the number of animals moving back to the dark area versus the number not doing so. The dark–light border zone was defined as a zone of one larval length between the dark and light area, such that two-thirds of the length are located in the dark area (r_{in}=r_{dark}−2/3 larval length≈6.9 mm for L1 and 39 mm for L3) and one-third is in the light area (r_{out}=r_{dark}+1/3 larval length≈8.6 mm for L1 and 44 mm for L3). The proportion of larvae that showed light avoidance behaviour at L1 versus L3 was compared with a two-tailed Z-test.

Video tracking of chemotaxis

Larvae were raised and staged as described above except that only 150–200 flies, of the w^{1118} genotype, were used for egg laying. Molasses–apple juice agarose plates with added yeast paste were used as a substrate. The larvae were collected and then briefly transferred onto an agarose Petri dish before testing.

The specifics of the chemotaxis assay and the tracking arena follow Gomez-Marin et al. (2011) (see also Louis et al., 2008a,b). In brief, the top part of a rectangular plastic lid (Falcon 353958 rectangular plate lid, Corning Inc., Corning, NY, USA) was coated with a layer of 3% agarose (SeaKem, LE Agarose, Lonza, Switzerland) to later serve as the base of the chemotaxis arena. Next, a solution of odour diluted in paraffin oil was pipetted into a single 9 mm well of a 96-well plate lid (Falcon 353071 lid for 96-well plates, Corning Inc.). For L3, 10 µl of ethyl butyrate (CAS: 105-54-4, Fluka; diluted to 30 mmol l^{-1} in paraffin oil, CAS: 8012-95-1, Sigma-Aldrich) was pipetted into one of the centrally located 9 mm wells. To adjust for the smaller size of L1, we used a custom-made well of only 3 mm diameter and reduced the volume of odour solution to 3 µl. We note that without these adjustments, and using Canton-Special larvae, poor chemotactic performance was observed in preliminary experiments with L1 (not shown). The plate lid with the odour droplet was flipped over and placed onto the agarose-coated lid, creating a closed behavioural arena with the odour-source lid at the top and the agarose-coated lid at the bottom. The arena remained closed for approximately 15 s, allowing an odour gradient to establish. Then, the top lid was briefly opened and a single larva was introduced into the centre of the bottom, agarose-coated lid. Tracking lasted for a maximum of 5 min and automatically ceased as soon as a larva left the field of view. The arena was illuminated from above by a flat light pad (Slimlite Lightbox, Kaiser, Buchen, Germany). We obtained and analysed 29 tracks for L1 and 23 tracks for L3. Reference measurements of locomotion of L1 were also performed in the absence of odour. Corresponding reference measurements in L3 were presented before (Gomez-Marin et al., 2011). In this no-odour condition, data were analysed relative to a 'fictive' odour located at the same position as the odour.

Behaviour was recorded at 5 frames s^{-1} with a video camera below the set-up. Tracking and image processing were performed with SOS-track software (Gomez-Marin and Louis, 2012; Gomez-Marin et al., 2012; Gomez-Marin and Louis, 2014). The positions of the head, tail, centroid and midpoint were extracted from every frame to calculate the kinematic variables of interest. Tracks were decomposed into runs and turns by the threshold rule of Gomez-Marin et al. (2011; see their fig. 2B); specifically, we set the threshold to identify the onset of a turning manoeuvre to a reorientation speed of 9 deg s^{-1} for L1 and to 12 deg s^{-1} for L3. To compare behaviour between L1 and L3, an odour gradient reconstructed for the L3 case (Gomez-Marin et al., 2011) was normalized and scaled by a factor of 3 to reflect the smaller diameter of the odour source used for the L1 case. Conclusions regarding chemotaxis of L1 remained unaltered if the original gradient was used for the analyses. That is, the scaling factor merely acts as a proxy for slight shape changes of the gradient in the set-up used for L1. Next, tracks were mapped onto the respective odour gradient to reconstruct the sensory experience of the larva as it moved about the arena. This way, the turn-triggered averages of the locally experienced odour concentration and the speed of the larva before and after turns could be computed. We calculated the probability of turning towards the left depending on the orientation of the larvae towards the odour source (bearing). According to convention, left turns reorient the larva towards the odour source when the bearing is larger than 0 deg; for bearings smaller than 0 deg, right turns reorient the larva towards the odour source. We relied on a bootstrap strategy to estimate a confidence interval in these turn probabilities

Journal of Experimental Biology (2017) 220, 2452-2475 doi:10.1242/jeb.156646

calculated on the full dataset; the standard error was calculated as described in Martinez and Martinez (2012). To see whether the curvature of a track is correlated with the direction to the odour source, weathervaning was quantified as described in Gomez-Marin and Louis (2014) through the instantaneous orientation rate separated across the bearing angle towards the odour source; error bars represent the confidence interval (95%) and were calculated by bootstrapping.

Immunohistology

Immunohistology related to odour–DAN activation associative learning

Males from the R58E02-Gal4 strain (Liu et al., 2012; Bloomington Stock Center no. 41347) were crossed to females homozygous for pJFRC2-10XUAS-IVS-mCD8::GFP (henceforth abbreviated as UAS-GFP; Pfeiffer et al., 2010; Bloomington Stock Center no. 32186). Larval tissues were dissected in phosphate-buffered saline (PBS) added with 10% normal goat serum and fixed for 30 min in 4% paraformaldehyde at room temperature. After multiple rinses in PBS with 1% Triton X-100 (PBS-TX), tissues were mounted on poly-lysine (CAS: 25988-63-0, Sigma-Aldrich)-coated coverslips, pre-blocked with 10% normal goat serum in PBS-TX for 30 min, and incubated in rabbit anti-GFP IgG (1:1000; ab290, Abcam, Atlanta, GA, USA) and mouse 1d4 anti-Fasciclin II (1:50; Developmental Studies Hybridoma Bank, Iowa City, IA, USA) in PBS-TX for 2 days at 4°C. After multiple rinses in PBS-TX, tissues were incubated for 2 days at 4°C with Alexa Fluor 488 goat anti-rabbit and Alexa Fluor 633 goat anti-mouse IgG (1:500; A-11008 and A-21052, respectively, Invitrogen, Carlsbad, CA, USA). Nervous systems were then washed 3 times in PBS-TX and mounted in antifade mountant (ProLong Gold, Molecular Probes, Eugene, OR, USA). Immunolabelled nervous systems were imaged on a Zeiss 710 confocal microscope using a 40× oil immersion objective (NA 1.4). Images of brains were assembled from a 2×1 array of tiled stacks, with each stack scanned as an 8-bit image with a resolution of 512×512 and a *z*-step interval of 1 µm.

Immunohistology related to rolling behaviour in response to optogenetic activation of basin interneurons

Males from the R72F11-Gal4 strain (Bloomington Stock Center no. 39786) were crossed to females of the strain 10xUAS-HA;CyO/Sp; MKRS/TM6 (henceforth abbreviated as UAS-HA; Nern et al., 2015). Brains were removed from L1 and fixed in PBS with 10% normal goat serum for 30 min in 4% paraformaldehyde at room temperature. After multiple rinses in PBS-TX, tissues were mounted on poly-lysine-coated coverslips (see above), pre-blocked with 10% normal goat serum in PBS-TX for 30 min, and incubated in rabbit anti-HA IgG (1:500; C29F4, Cell Signaling Technology, Danvers, MA, USA) and mouse 1d4 anti-Fasciclin II (1:50; Developmental Studies Hybridoma Bank) in PBS-TX for 2 days at 4°C. After multiple rinses in PBS-TX, tissues were incubated for 2 days at 4°C with Alexa Fluor 488 goat anti-rabbit and Alexa Fluor 633 goat anti-mouse IgG (1:500; A-11008 and A-21052, respectively, Invitrogen). Nervous systems were then washed 3 times in PBS-TX and mounted in antifade mountant (ProLong Gold, Molecular Probes). Immunolabelled nervous systems were imaged on a Zeiss 710 confocal microscope using a 63× oil immersion objective (NA 1.4).

Immunohistology related to stability and dynamics of transgene expression across larval stages

Males from the indicated Gal4 strains (Li et al., 2014; R16F06-Gal4, R26G02-Gal4, R53F05-Gal4, R68B06-Gal4; Bloomington Stock Center nos 48734, 48065, 50440, 39458) were crossed to females homozygous for P{10XUAS-IVS-mCD8::GFP}attP40 (Pfeiffer et al., 2010; Bloomington Stock Center no. 32186). Larval tissues were dissected in PBS and fixed for 1 h in 4% formaldehyde in PBS at room temperature. After multiple rinses in PBS-TX, tissues were mounted on poly-lysine-coated coverslips (see above), pre-blocked with 3% normal donkey serum in PBS-TX for 1 h, and incubated in the following primary antibodies: rabbit anti-GFP IgG (1:1000; A11122, Invitrogen), mouse anti-Neuroglian (1:50; BP104, Developmental Studies Hybridoma Bank) and rat anti-N-cadherin (1:50; DN-Ex 8, Developmental Studies Hybridoma Bank) in PBS-TX for 2 days at 4°C. After multiple rinses in PBS-TX, tissues were incubated for 2 days at 4°C with the following secondary antibodies, all at 1:500 dilution and obtained from Jackson ImmunoResearch (West Grove, PA, USA): AlexaFluor 488-conjugated donkey anti-rabbit (711-545-152), AlexaFluor 594-conjugated donkey anti-mouse IgG (715-585-151) and AlexaFluor 647-conjugated donkey anti-rat IgG (712-605-153). Nervous systems were then washed 2–3 times in PBS-TX, dehydrated through a graded ethanol series, cleared in xylene and mounted in DPX (Sigma-Aldrich). Immunolabelled nervous systems were imaged on a Zeiss 510 confocal microscope using a 40× oil immersion objective (NA 1.3). Images of each nervous system were assembled from a 2×3 array of tiled stacks, with each stack scanned as an 8-bit image with a resolution of 512×512 and a *z*-step interval of 2 µm.

All experiments and analyses comply with applicable ethical regulations and law. The data underlying the presented figures and used for statistical analyses are documented in Table S1. Assuming effect sizes were equal or moderately less in L1 relative to data published for L3, sample sizes were chosen to be equal to or slightly higher than previously published sample sizes for L3.

RESULTS

We first present the results of the counting-based assays, followed by the results from the assays based on video tracking.

Olfactory and gustatory preference

L1 and L3 showed attraction to both odours tested (*n*-amyl acetate and 1-octanol; Fig. 1A,B), in line with what has previously been reported for L3 (e.g. Cobb, 1999; Saumweber et al., 2011). For both odours, it took slightly longer for this preference to become significant for L1. The same pattern of results was observed for the gustatory preference behaviour for fructose and arabinose (Fig. 2A,B); for sorbitol, preference did not reach significant levels in L1 during the observation period (Fig. 2C). We note that the early, transient aversiveness of sorbitol in L3 was not observed in L1. Preference for various sugars has previously been reported for L3 (e.g. Schipanski et al., 2008; Rohwedder et al., 2012).

Avoidance of quinine in L1 was consistently less than in L3, but converged towards the same level at the end of the observation period, suggesting that it took longer for L1 to reach these levels (Fig. 2D). Avoidance of quinine has previously been reported for L3 (e.g. El-Keredy et al., 2012).

Preference scores for aspartic acid were low in both L1 and L3; indeed, only after 16 min did weak attraction to aspartic acid become evident in L3 (Fig. 2E), an effect that failed to reach significance for L1. Attraction to aspartic acid has previously been reported for L3 (Croset et al., 2016), and using a modified assay geometry for both L1 and L3 (Kudow et al., 2017).

Thus, for the odours and tastants tested above, the general result is that these cues have concordant valence for the two larval stages and that it takes slightly longer until the same levels of preference are

Journal of Experimental Biology (2017) 220, 2452-2475 doi:10.1242/jeb.156646

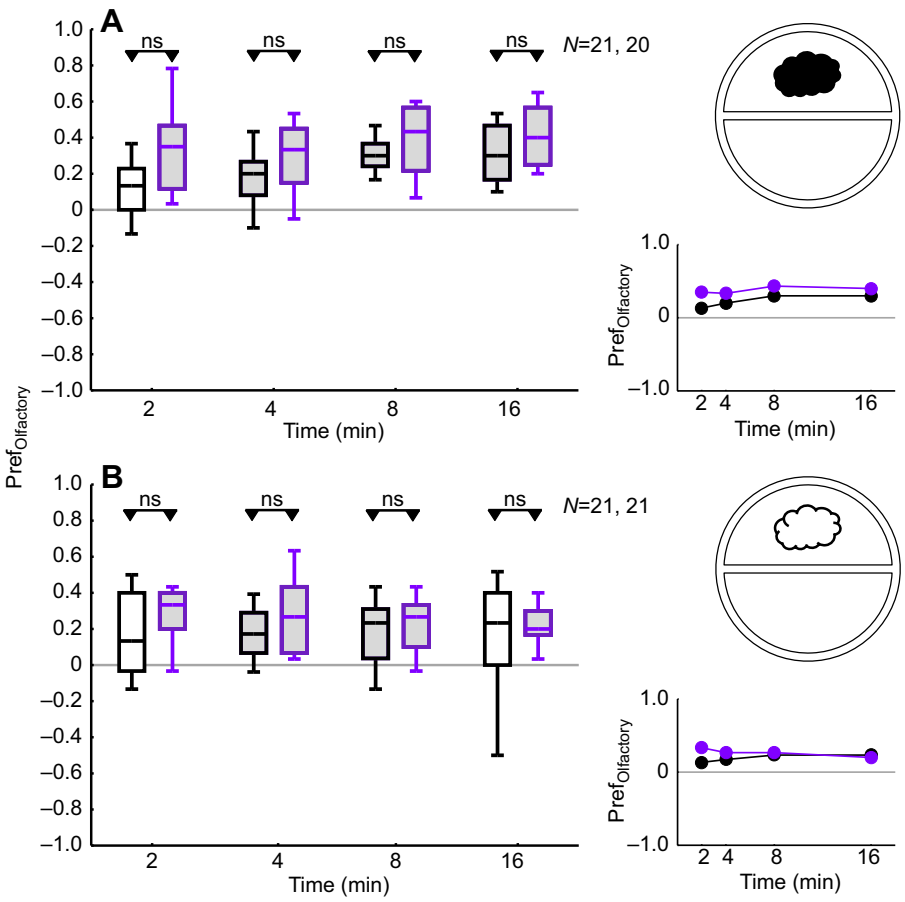

Fig. 1. Olfactory preference. (A) Larvae were allowed to choose between one side of a Petri dish that featured a container filled with *n*-amyl acetate (1:50) as odour (black cloud) and the other side, which did not. An olfactory preference index ($Pref_{Olfactory}$) was calculated for the distribution of larvae 2, 4, 8 and 16 min after the experiment had started. Positive values indicate attraction to *n*-amyl acetate, which is statistically significant after 2 min for stage 3 larvae (L3, magenta box plots), while this is the case only after 4 min for stage 1 larvae (L1, black box plots). In direct comparisons, attraction to *n*-amyl acetate in L1 is not significantly less than that in L3 at any time point. The inset presents the median of the preference indices plotted over time. (B) As in A, but using 1-octanol (pure; white cloud) as odour. Preference for 1-octanol is statistically uniform in L1 and L3. The box plots show the median, 25% and 75% quantiles as the box boundaries, and 10% and 90% quantiles as whiskers. ns refers to Bonferroni-corrected Mann–Whitney *U*-test (MWU) comparisons between groups ($P<0.05/4$); grey shading of the box plots indicates Bonferroni-corrected within-group significance from zero in one-sample sign tests (OSS) ($P<0.05/4$). Sample sizes (N) are given within the figure.

reached for L1 as compared with L3. One simple explanation of these results is that L1 are smaller and slower in locomotion than L3. Such slower locomotion cannot, however, account for the results obtained for salt that are presented in the next section.

It has previously been reported for L3 as well as for adult *Drosophila* that low salt concentrations are moderately attractive, while high concentrations are strongly aversive; at intermediate concentrations, these behavioural tendencies cancel each other out (Niewalda et al., 2008; Russell et al., 2011). This inverted U-shaped dose–effect function for salt preference behaviour may be shifted towards the left, i.e. towards higher sensitivity, in L1: that is, both attraction at low concentrations and avoidance at high concentrations of salt are stronger in L1 (Fig. 2F–H). Obviously, slower locomotion in L1 works against such stronger attraction/avoidance scores, such that the valence differences for salt between L1 and L3 may actually be underestimated.

Thus, olfactory and gustatory preference behaviour in L1 and L3 is essentially equal in valence and strength – although it takes longer for L1 to express these preferences – except in the case of salt, where a shift towards higher sensitivity may occur in L1 (see Fig. S1 for a summary).

Odour–tastant associative learning

It has previously been reported for L3 that repeatedly presenting an odour together with a fructose reward increases preference for the odour in a subsequent test (Scherer et al., 2003; Neuser et al., 2005; Saumweber et al., 2011). Specifically, in one group of larvae, the odour *n*-amyl acetate (AM) is presented together with fructose as a reward (+) and 1-octanol is presented without a reward (AM+/OCT), while a second group of larvae undergoes reciprocal training (AM/OCT+). Then, animals are tested for their choice between AM versus OCT in the absence of the fructose reward. Appetitive associative memory is indicated by a relatively higher preference for AM after AM+/OCT training compared with the reciprocal AM/OCT+ training. This difference in preference is quantified by the associative PI, such that positive PIs indicate appetitive associative memory (and negative PIs indicate aversive memory). The elevated preference for the reward-associated odour can be grasped as a memory-based search for that reward, because it ceases if the sought-for reward is actually present during the test (Gerber and Hendel, 2006; Saumweber et al., 2011; Schleyer et al., 2011, 2015a,b; see also Schleyer et al., 2013).

As previously reported for L3, odour–fructose training also established appetitive memory in L1 (Fig. 3A1, left box plot for the associative PIs; and Fig. 3A2, the two left box plots for the underlying preference scores) (see also Pauls et al., 2010). Notably and also as previously observed for L3, the associative preference for the fructose-associated odour was abolished if the test was performed in the presence of the fructose reward (Fig. 3A1,A2, right box plots).

Likewise, as previously reported for L3 (Schleyer et al., 2015a), odour–aspartic acid training established appetitive memory in L1, a memory that can be prevented from behavioural expression by the presence of aspartic acid during the test (Fig. 3B).

To provide a case of taste–punishment learning, we trained L1 by presenting one of the odours together with quinine, while the other odour was presented alone. As previously reported for L3 (Gerber and Hendel, 2006; Schleyer et al., 2011, 2015a; El-Keredy et al., 2012), no learned behaviour towards the quinine-associated odour was observed (Fig. 3C1, left box plot for the associative PIs; and Fig. 3C2, the two left box plots for the underlying preference scores)

Journal of Experimental Biology (2017) 220, 2452-2475 doi:10.1242/jeb.156646

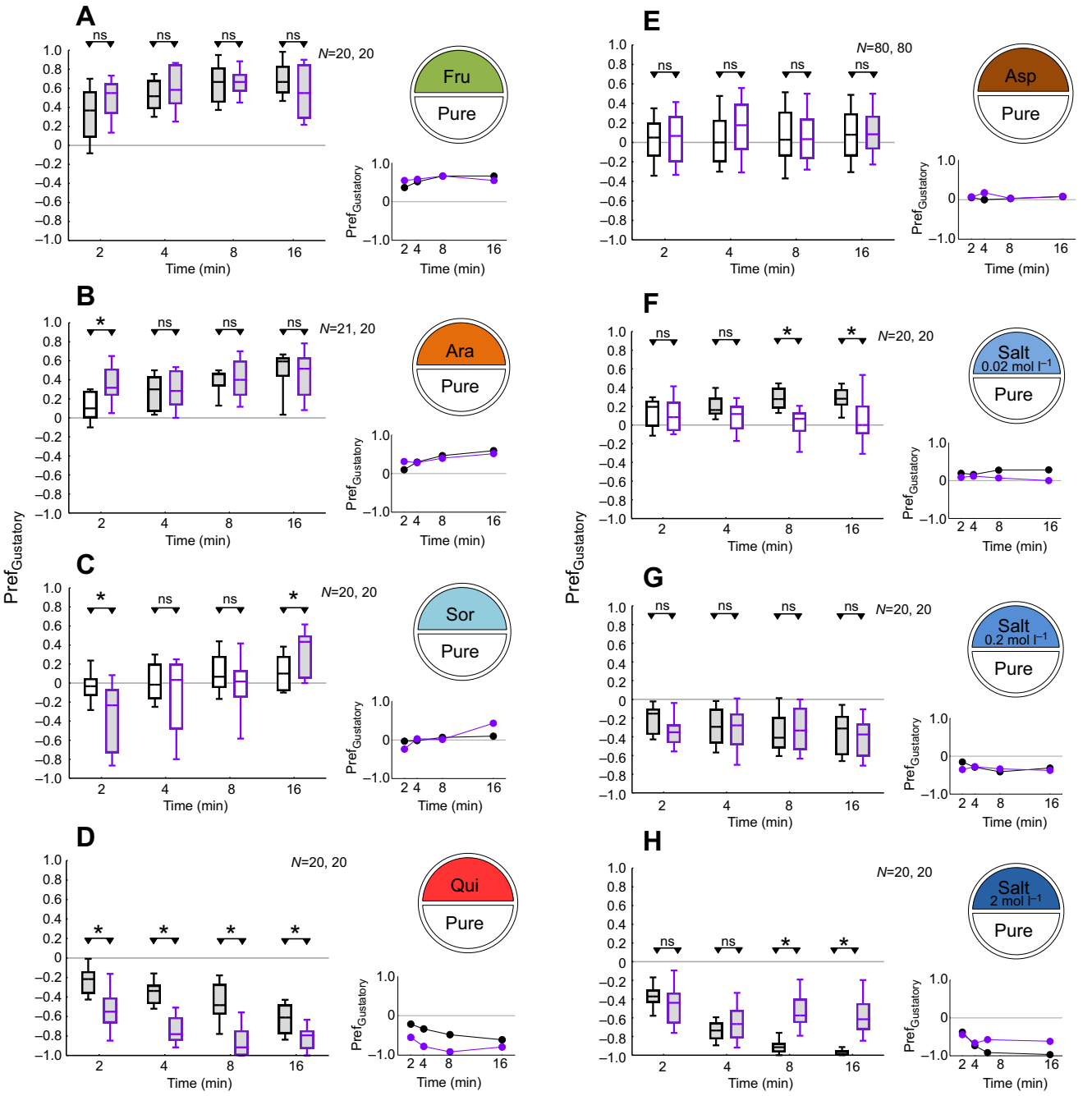

Fig. 2. Gustatory preference. (A) Larvae were allowed to choose between one side of a Petri dish that contained pure agarose (pure) and the other side, which contained agarose with 2 mol l^{-1} fructose (Fru). A gustatory preference index ($Pref_{Gustatory}$) was calculated for the distribution of the larvae 2, 4, 8 and 16 min after the experiment had started. Positive values indicate attractiveness of fructose, which is statistically significant from 2 min for both L1 (black box plots) and L3 (magenta box plots). Attractiveness of fructose in L1 is not significantly less than that in L3 at any time point. The inset presents the median scores plotted over time. (B) As in A, but using 2 mol l^{-1} arabinose (Ara). Attraction of arabinose is statistically significant from 4 min on for L1, and after 2 min for L3. Attraction of arabinose in L1 is less than that in L3 early on, i.e. after 2 min, but not at the other time points. (C) As in A, but using 2 mol l^{-1} sorbitol (Sor). L1 were indifferent towards sorbitol at all time points; L3 showed a slight yet significant avoidance at 2 min and attraction after 16 min. At that last time point, preference scores in L3 were higher than those for L1. (D) As in A, but using 5 mmol l^{-1} quinine (Qui). Avoidance of quinine is statistically significant from 2 min for both L1 and L3. Avoidance of quinine in L1 is less than that in L3 at all time points. (E) As in A, but using 10 mmol l^{-1} aspartic acid (Asp). Attraction to aspartic acid is not statistically significant for any of the time points except for L3 at 16 min. Scores do not differ between L1 and L3 at any time point. (F–H) As in A, but using a low, intermediate or high concentration of salt (NaCl: 0.02, 0.2 or 2 mol l^{-1}, respectively). (F) For L1, attraction to the low concentration is statistically significant from 4 min on, while for L3, only tendencies for attraction are observed. At 8 and 16 min, L1 show stronger attraction than L3. (G) For an intermediate concentration of salt, both L1 and L3 larvae show aversion, and do so to the same extent for all time points. (H) For the high salt concentration, avoidance is statistically significant at all time points for both L1 and L3. At 8 and 16 min, L1 show stronger aversion than L3 and ns refer to Bonferroni-corrected MWU comparisons between groups ($P<0.05/4$); grey shading of the box plots indicates Bonferroni-corrected within-group significance from zero in OSS tests ($P<0.05/4$). Sample sizes are given within the figure.

Journal of Experimental Biology

Journal of Experimental Biology (2017) 220, 2452-2475 doi:10.1242/jeb.156646

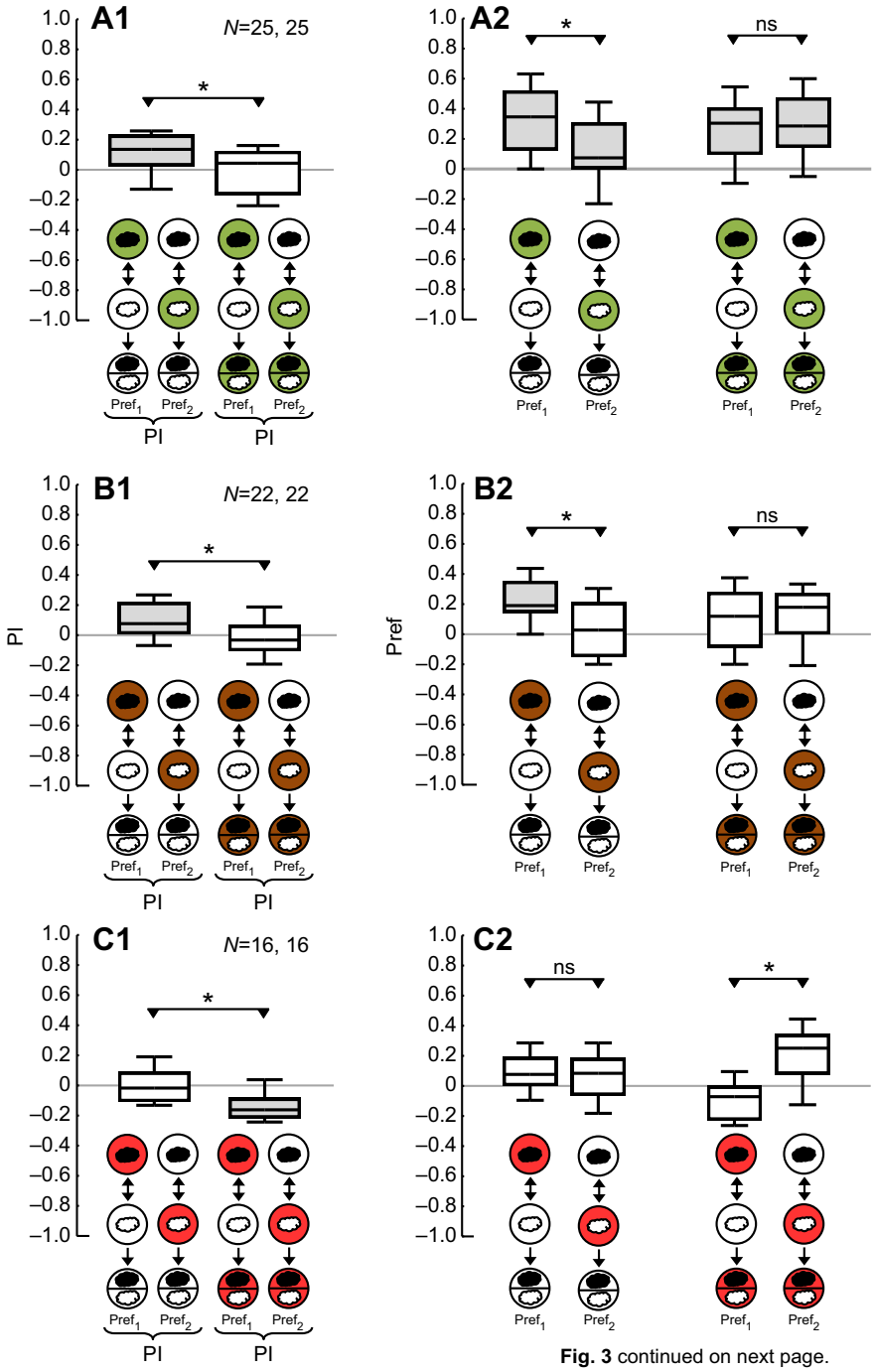

Fig. 3 continued on next page.

Fig. 3. Odour–tastant associative learning. (A) Fructose as reward in L1. One set of L1 received one odour (*n*-amyl acetate, black cloud) paired with a 2 mol l^{-1} fructose reward (green fill of Petri dish), and the other odour (1-octanol, white cloud) with pure agarose (white fill of Petri dish); the second set of L1 received reciprocal training (*n*-amyl acetate without reward and 1-octanol with reward). Testing of the choice between the two odours was performed either in the absence of the fructose reward, i.e. on pure agarose plates (shown below left box plot in A1) or in the presence of the fructose reward (shown below right box plot in A1). Appetitive associative memory is indicated by positive performance indices (PIs), showing that larvae systematically prefer the previously rewarded over the previously non-rewarded odour [the underlying preference (Pref) scores are presented in A2, such that preference for *n*-amyl acetate yields positive scores]. Associative PIs are significant in the absence but not in the presence of the fructose reward. This indicates that appetitive associative memory supports learned search behaviour, which is only expressed in the absence of the sought-for fructose reward. (B) As in A, but using 10 mmol l^{-1} aspartic acid (brown) as a reward. Aspartic acid memory is only expressed in the absence but not in the presence of aspartic acid. (C) As in A, but using 5 mmol l^{-1} quinine (red) as a punishment. Aversive associative memory is indicated by negative PIs. Notably, quinine memory is only expressed in the presence but not in the absence of quinine, i.e. it is a form of learned escape. (D,E) Salt as punishment in L1 but as reward in L3. As in A, but using 0.2 mol l^{-1} sodium chloride (blue). Notably, L1 show aversive memory in the presence but not the absence of this salt concentration (D), while L3 show appetitive memory in the absence but not the presence of salt (E). It thus seems that the dose–effect function for salt reinforcement in L3, from rewarding at low salt concentrations to punishing at high salt concentrations (Niewalda et al., 2008; Russell et al., 2011), is shifted towards the left in L1, i.e. towards higher sensitivity. Thus, a salt concentration that is rewarding to L3 is punishing to L1. * and ns refer to MWU comparisons between groups (A1–E1: *P<0.05; A2–E2: * or ns P< or >0.05/2); grey shading of the box plots indicates Bonferroni-corrected within-group significance from zero in OSS tests (A1–E1: P<0.05/2; A2–E2: P<0.05/4). Sample sizes are given within the figure.

Journal of Experimental Biology (2017) 220, 2452-2475 doi:10.1242/jeb.156646

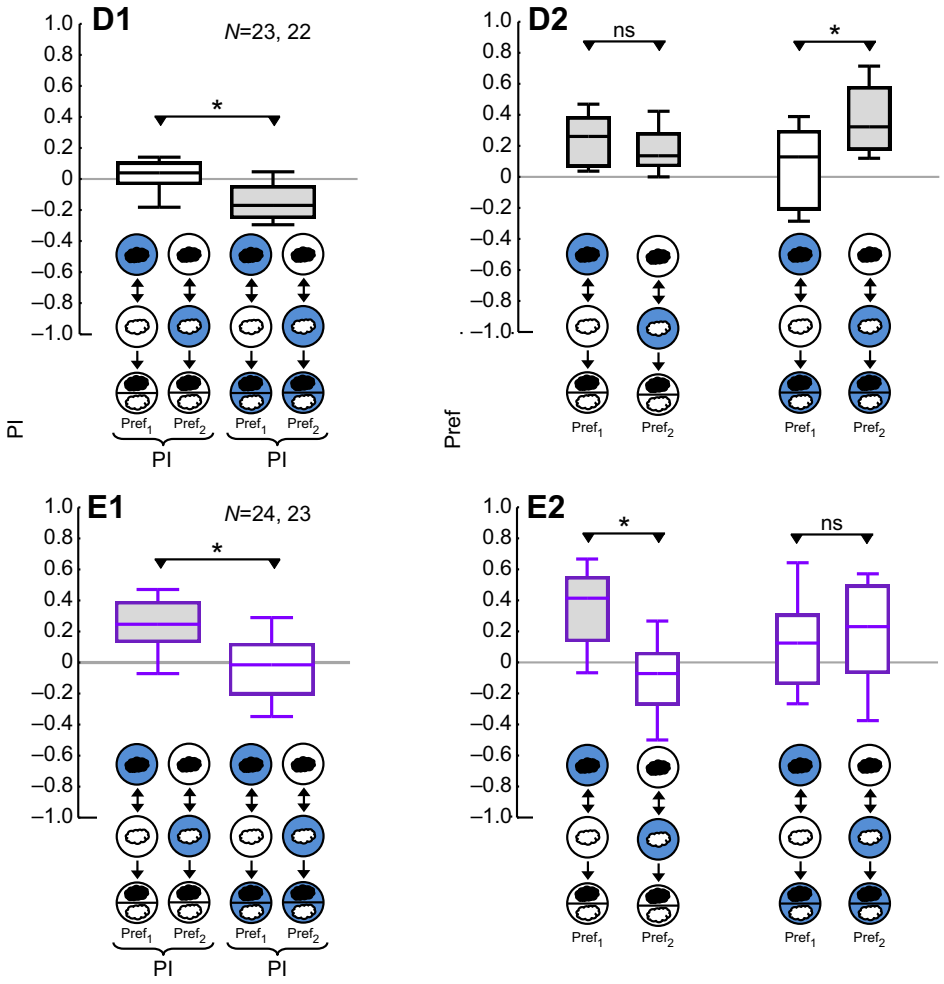

Fig. 3. (Continued)

unless quinine was present during the test (Fig. 3C1, right box plot for the associative PIs; and Fig. 3C2, the two right box plots for the underlying preference scores). This arguably is because learned behaviour after odour–punishment training is a form of learned escape that is behaviourally expressed only if the testing situation does indeed require escape.

The case of odour–salt associative learning turned out to be special. In L3, it was previously found that low concentrations of salt have a rewarding effect, while high concentrations of salt are punishing (Niewalda et al., 2008; Russell et al., 2011). Using 0.2 mol l^{-1} NaCl – a concentration that was reported to be rewarding in L3 – we were surprised to observe aversive memory in L1. That is, when tested in the absence of salt, associative PIs were zero, while negative scores were uncovered when testing was carried out in the presence of salt (Fig. 3D). As mentioned in the preceding paragraph for quinine, this can be seen as a case of learned escape from the salt-associated odour that is warranted only when the salt to escape from is actually present. Thus, a salt concentration that is punishing in L1 is rewarding in L3 (for a confirmation of the latter result under the present conditions, see Fig. 3E). Possibly, the inverted U-shaped dose–effect function for salt as a reinforcer, from rewarding at low concentrations to punishing at high concentrations, is shifted towards the left for L1, i.e. towards higher sensitivity. Such an interpretation would also fit the results regarding salt preference behaviour presented in the preceding section (Fig. 2F–H). Likely explanations for such a generally increased sensitivity to salt are that the geometry of L1 renders them more susceptible to osmotic stress by high salt concentrations in the substrate, and/or that their cuticle is less protective for such osmotic stress. Indeed, salt concentrations high enough to be punishing in L3 are lethal for L1 (data not shown).

We note that for L3, the dose–effect function for the reinforcing effect of salt was reported to be shifted rightward along the concentration axis relative to preference behaviour (Niewalda et al., 2008; Russell et al., 2011). In other words, for salt to be an effective punishment, a higher concentration is needed than is required to induce avoidance. This was confirmed within the present study: a salt concentration that L3 avoided in a preference test (0.2 mol l^{-1}; Fig. 2G) was not punishing to them, but instead was rewarding (Fig. 3E).

Thus, the faculties for odour–taste associative learning, and the rules for behaviourally expressing the established memories, are strikingly similar for L1 when compared with previous reports concerning L3. The exception to this rule is salt, as apparently L1 are much more sensitive to salt reinforcement than L3.

Odour–DAN activation associative learning

It has been reported for L3 that repeatedly presenting an odour together with optogenetic activation of R58E02-Gal4-positive DANs associatively increases preference for the odour in a subsequent test (Rohwedder et al., 2016). Specifically, in one

Journal of Experimental Biology (2017) 220, 2452-2475 doi:10.1242/jeb.156646

group of larvae, the odour ethyl acetate (EA) is presented paired with red light for optogenetic DAN activation (*), alternated with blank trials (EA*/blank training). A second group of larvae receives unpaired presentations of odour and red light (EA/* training). Then, all animals are tested for their preference for EA. Appetitive associative memory is indicated by a relatively higher preference for EA after paired EA*/blank training compared with unpaired EA/* training. This difference in preference is quantified by the associative PI, such that positive PIs indicate appetitive associative memory (negative PIs would indicate aversive memory).

The present results show that odour–DAN activation training also established appetitive memory in L1 (Fig. 4A for the associative PI of the experimental as well as the effector and driver control strains; Fig. 4B for the underlying preference scores). Thus, activation of the R58E02-Gal4 DANs was also sufficient as an internal reward signal in L1. Interestingly, the R58E02-Gal4 driver labels three DANs of the pPAM-cluster in L3, respectively innervating the shaft, and upper and intermediate toe of the mushroom body medial lobe (Rohwedder et al., 2016). However, only two such cells were labelled in L1 (Fig. 4C, arrows; occasionally, an additional cell was

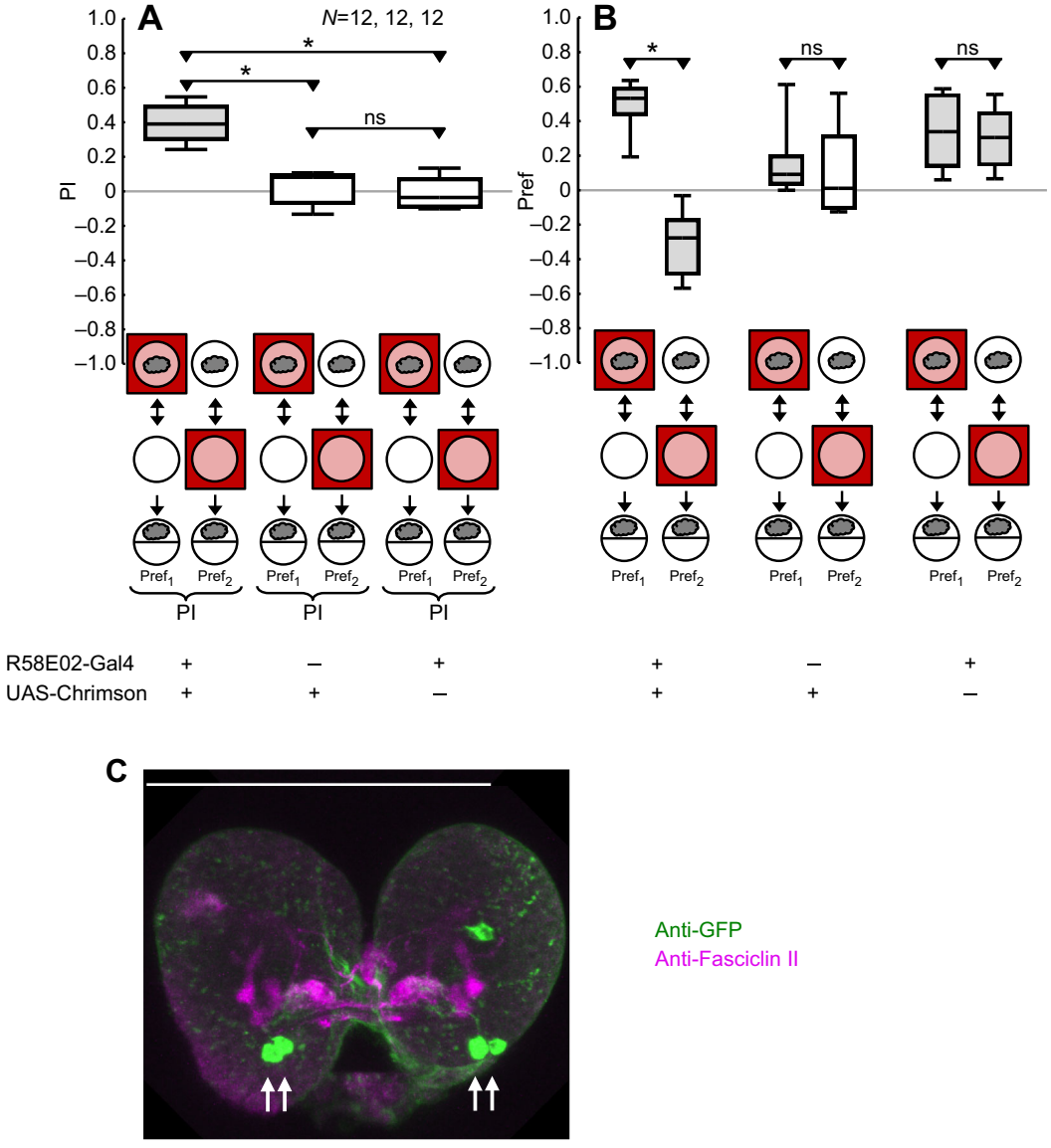

Fig. 4. Odour–DAN activation associative learning. (A) Dopaminergic neuron (DAN) activation as a reward in L1. One set of L1 received odour (ethyl acetate, grey cloud) paired with red light for optogenetic DAN activation (red square around Petri dish), alternated with blank trials (white-filled Petri dish); the second set received unpaired odour and red light. In both groups, this training was followed by a test of odour preference. Appetitive associative memory is indicated by positive PIs, reflecting that larvae have a systematically higher preference for the odour after paired rather than unpaired training. For the experimental genotype expressing Chrimson in the R58E02-Gal4 DANs, positive PIs are observed, showing that DAN activation is sufficient as an internal reward signal. In the effector and the driver control genotypes, the DANs are not activated and PIs are indistinguishable from chance levels. (B) Preference scores (Pref) underlying the PIs from A. * and ns refer to Bonferroni-corrected MWU comparisons between groups (A,B: $P<$ or $>0.05/3$); grey shading of the box plots indicates Bonferroni-corrected within-group significance from zero in OSS tests (A: $P<0.05/3$; B: $P<0.05/6$). (C) Anti-GFP visualization in R58E02-Gal4×UAS-GFP L1 (green) (expression from R58E02-Gal4 in L3 has recently been described by Rohwedder et al., 2016). Expression of GFP can be discerned in two pPAM-cluster neuron cell bodies in each hemisphere (arrows) projecting onto the mushroom bodies revealed through anti-Fasciclin II detection (magenta). For a tentative identification of these cells as DAN-i1 and DAN-j1, see Results; occasionally, and as can be seen in the current preparation, an additional cell was observed which did not innervate the mushroom bodies. The scale bar represents 100 µm. Sample sizes are given within the figure.

Journal of Experimental Biology

Journal of Experimental Biology (2017) 220, 2452-2475 doi:10.1242/jeb.156646

observed which did not innervate the mushroom bodies). Specifically, L3 R58E02-Gal4 larvae express in DAN-h1, -i1 and -j1 (Rohwedder et al., 2016; nomenclature according to Eichler et al., 2017). Given that Eichler et al. (2017) found that of these DANs only DAN-h1 is not present in an L1 whole-brain electron microscope volume, the two mushroom body-innervating cells labelled in Fig. 4C in an L1 are tentatively identified as DAN-i1 and DAN-j1.

Light/dark–electric shock associative learning

L1 were trained either with light paired with electric shock and darkness without shock or with light-alone trials and darkness paired with electric shock punishment. This was followed by a test of their light–dark preference (see Fig. 5A). L1 behaved the same regardless of the previous training regimen in this test; that is, PIs were zero (Fig. 5A, left box plots). Correspondingly, light–dark preference scores were equal between the reciprocally trained groups of L1 and indicated avoidance of light (Fig. 5B, left box plots). This result was surprising, given the previously reported learning of L3 in a similar paradigm (von Essen et al., 2011). We therefore ran the current paradigm for L3 too, and confirmed their light/dark–electroshock learning ability (Fig. 5A). Indeed, avoidance of light was stronger after the light had been paired with an electric shock as compared with the reciprocally trained group of L3 (Fig. 5B, middle box plots); no such alteration was seen when the shock was omitted during training, arguing that these differences in light avoidance are associative in character and are unrelated to the difference in the duration of light–dark exposure between reciprocal groups (Fig. 5A,B, right box plots).

Food intake

Larval feeding behaviour has been measured in different assays (e.g. Bjordal et al., 2014; Gasque et al., 2013; Neckameyer, 2010; Schoofs et al., 2014). In particular for short-term food intake assays, choosing the appropriate duration of the experiment is crucial. We therefore determined food intake in L1 at different time points, and compared the changes in food ingested over time with values for L3 (Fig. S2A). We found the time course of food intake across the assay duration to be virtually identical for L1 and L3 (Fig. S2B). For both stages, the largest increase in food uptake occurred between 10 and 20 min, making 20 min the experimental duration most likely to enable detection of changes in food intake in this assay.

Burrowing

When allowed 60 min to feed, roam around or burrow into the substrate of a Petri dish containing yeast diet, it took L1 longer to burrow into the substrate than L3. That is, while half of the L3 had already burrowed into the substrate after 5 min, L1 took about 10 times longer to reach this point (Fig. S3).

Mechano-nociception and touch

We aimed at applying a stimulus to L1 and L3 that was noxious but not damaging. This is not trivial, as the cuticle is softer in L1 and therefore noxious stimuli normally used for L3 (30–100 mN) frequently cause tissue damage to L1. We therefore calibrated stimulation to a force of 20 mN for L1 and 50 mN for L3. Under such conditions of different physical stimulation adjusted to be not physically damaging for either stage, both L1 and L3 showed the previously characterized types of behaviour towards noxious

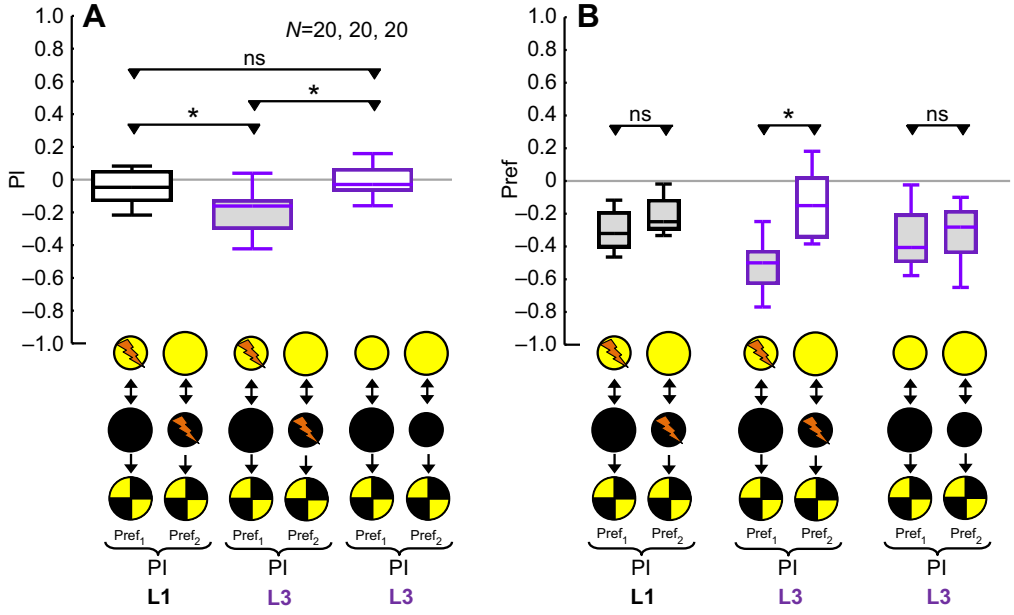

Fig. 5. Light/dark–electric shock associative learning. One group of larvae received light exposure (yellow fill of circles) paired with an electroshock punishment (100 V; lightning symbol), and darkness (black fill of circles) without electroshock (light+/dark training). A second group of larvae received light/dark+ training. Circles indicate agarose-filled Petri dishes; the smaller diameter circles represent a 1 min trial duration, while the larger diameter circles indicate a 5 min trial duration. During the test, the preference of the larvae for the lit quadrants was determined. (A) The performance index (PI) quantifies the difference in light preference between the two groups, such that negative PIs reflect avoidance of the shock-paired visual condition. (B) The underlying preference scores (Pref), such that preference for the lit quadrants yields positive scores. Experiments were performed with either L1 (black box plots) or L3 (magenta box plots). Given that total light exposure was not equal between groups (see Materials and methods), a control experiment was performed in L3 by subjecting them to training-like handling and light exposure, but omitting all electroshocks (rightmost condition in A and B). L1 do not show avoidance of the shock-associated visual condition, while L3 do. As shown for L3, differences in light exposure are not sufficient to lead to differences in light avoidance, arguing that the negative PIs observed reflect associative memory. * and ns refer to MWU comparisons between groups (P<0.05/3); grey shading of the box plots indicates Bonferroni-corrected within-group significance from zero in OSS tests (A: P<0.05/3; B: P<0.05/6). Sample sizes are given within the figure.

Journal of Experimental Biology

Journal of Experimental Biology (2017) 220, 2452-2475 doi:10.1242/jeb.156646

stimuli, namely stop, stop and turn, bending, and rolling, and did so at about the same proportions (Fig. 6A). Only rolling, the strongest nociceptive behaviour, was tendentially less likely to occur in L1 under the chosen conditions (Fig. 6A, right bars); note that arguably rolling is a nocidefensive rather than nociceptive behaviour.

Upon gentle touch with an eyelash, both L1 and L3 showed the typical behavioural signs of disturbance (Kernan et al., 1994), at

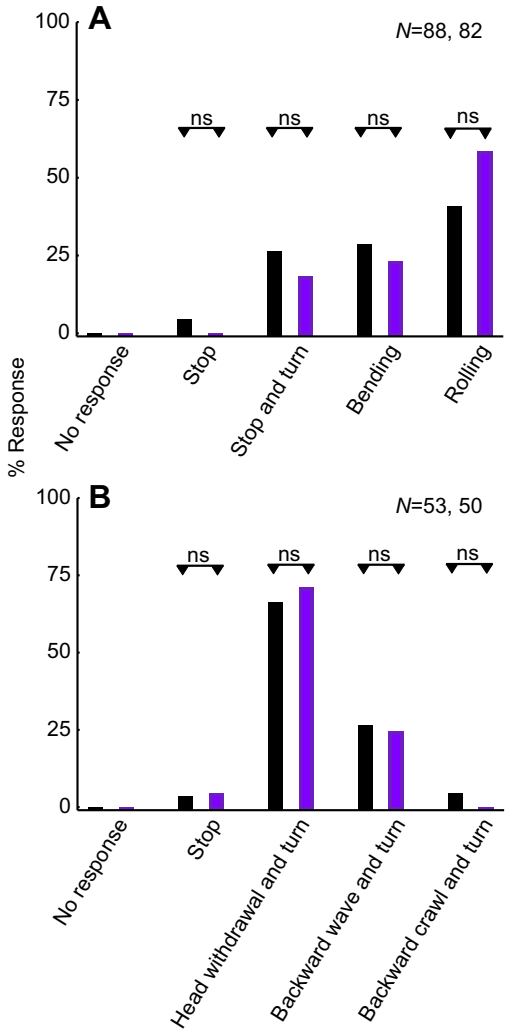

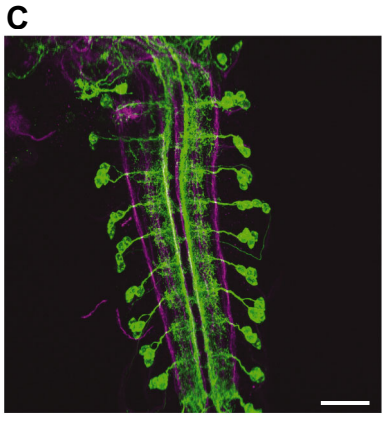

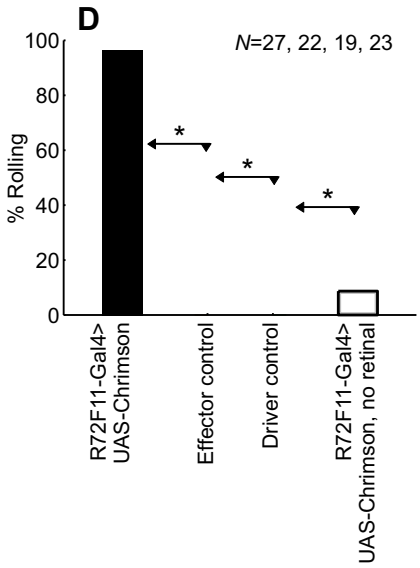

Fig. 6. Mechano-nociception and touch. (A) Mechano-nociception. Shown are the responses of L1 (black bars) and L3 (magenta bars) to a mechano-nociceptive stimulus adjusted to be just-not damaging for either stage (L1: 20 mN, L3: 50 mN). L1 and L3 display nociceptive behaviour (bending, rolling) as well as non-nociceptive behaviour (stop, stop and turn) at the same rates. ns refers to Bonferroni-corrected two-tailed *Z*-tests between L1 and L3 ($P>0.05/4$) (XLSTAT, Statcon, Witzenhausen, Germany). (B) Gentle touch. Shown are the responses of L1 (black bars) and L3 (magenta bars) to an innocuous mechanical stimulus (brush with eyelash). L1 and L3 exhibit behavioural signs of mild disturbance (stop, head withdrawal and turn, backward wave and turn, backward crawl and turn) at the same rates. ns refers to Bonferroni-corrected two-tailed *Z*-tests between L1 and L3 ($P>0.05/4$) (XLSTAT, Statcon). (C,D) Rolling in response to optogenetic activation of basin interneurons. C shows anti-HA visualization from a R72H11×UAS-HA L1 (green). Expression of HA can be discerned in the basin interneurons of the ventral nerve cord; longitudinal fibre bundles stained for anti-Fasciclin II (magenta) allow orientation in the preparation. Scale bar, 25 µm. In D, L1 of the indicated genotypes were stimulated with light and scored for rolling behaviour. L1 of the experimental genotype expressing Chrimson in the basin interneurons are likely to show rolling upon light stimulation, while larvae of the genetic controls, or larvae of the experimental genotype raised without retinal (open bar), are not. *$P<0.05/3$ in Bonferroni-corrected two-tailed *Z*-tests between the experimental genotype raised with retinal versus the respective control condition (XLSTAT, Statcon). Sample sizes are given within the figure.

Journal of Experimental Biology (2017) 220, 2452-2475 doi:10.1242/jeb.156646

about the same proportions. That is, in the large majority of cases, animals from both stages showed withdrawal of the head followed by turning, or a single backward wave of body peristalsis which then was also followed by turning (Fig. 6B).

To further investigate rolling behaviour, we optogenetically activated the somatosensory basin interneurons (Fig. 6C) in L1. Crossing the R72F11-Gal4 driver strain with the UAS-Chrimson effector strain and raising larvae in food supplemented with retinal for proper function of the Chrimson protein, we observed rolling behaviour in 95% of animals in response to light stimulation (Fig. 6D). This fits with what has previously been reported for L3 (Ohyama et al., 2015). No rolling was seen in the genetic control strains, and only very rarely if retinal was omitted from the larval diet. Movie 1 presents examples of optogenetically induced rolling behaviour in L1 and L3.

Video tracking of the response to 'buzz' mechanosensory disturbance

We measured translational run speed as well as the angular sideways speed of L1 and L3, both under baseline conditions and upon presentation of a disturbing mechanosensory 'buzz' stimulus (Eschbach et al., 2011; Saumweber et al., 2014). Under baseline conditions, translational run speed was about 4-fold lower in L1 than in L3, while angular speed was equal in the two stages (Fig. S4A,B). In other words, L1 ran slower, but sideways movements and turns were of the same speed as in L3. In order to compare the buzz-induced changes in translational run speed and angular speed between stages, we normalized these measures, for each larva, to those obtained immediately before the buzz. These normalized measures of translational run speed and angular speed did not reveal a difference between L1 and L3 (Fig. S4C,D). Both stages became hunched and slowed down (i.e. they showed a 'startle' response) for 2–3 s after the buzz; during the first few seconds, they typically implemented sideways movements (see also Movie 4).

Video tracking of 'free' locomotion

In Fig. 7A and in Movies 2 and 3, we show example tracks of locomotion for L1 and L3. As previously reported (Otto et al., 2016), larval locomotion alternated between go and reorientation phases.

Qualitatively, body contractions and the resulting peristalsis during go-phases appeared to be less regular in L1 than in L3 (Fig. 7B; Movie 2). Quantitatively, the frequency of peristaltic contractions during go-phases was about 20% higher for L1 than for L3 (Fig. 7C). As expected from their smaller body size, the absolute speed during go-phases was much slower for L1 than for L3 (Fig. 7D; see also Fig. S4A). Notably, from a 4-fold difference in absolute speed during go-phases, very little difference remained when considering speed relative to body length (Fig. 7E).

L1 were much more likely to be observed in a bent body posture than L3 (Fig. 7F); for example, L1 were found to be bent by 30 deg or more in about 30% of the frames, while for L3 this was the case for only 10% of all frames. Also, turn rate was much higher in L1 than in L3 (Fig. 7G). In effect, L1 gained less relative distance from their site of origin than L3 (Fig. 7H). This reduced 'exploration range' in L1, even when normalized to body length, manifests largely as differences in bending and turning behaviour (Fig. 7F,G), rather than in speed (Fig. 7E).

Video tracking of thermotaxis

Both L1 and L3 crawled away from their starting position at the hot 33°C isothermal line and reduced their distance to the colder side linearly during the observation period (Fig. 8A,B; Movie 5). While navigating away from the heat, L1 and L3 showed a median bearing of about 62 and 58 deg towards the cold side, respectively (Fig. 8C). In other words, L1 and L3 are typically oriented obliquely to the isothermal lines of 29 and 18°C, respectively, with L1 doing slightly higher-amplitude zig-zagging during go-phases and being oriented towards the 'wrong', hot side slightly more often.

Absolute speed of L1 in the heat gradient was about 3-fold lower than that of L3 (Fig. 8D); when considering speed normalized to body length, however, L1 appeared to move faster (Fig. 8E). Indeed, when comparing speed under free-crawling conditions versus in the heat gradient, speed was approximately 50% higher in the heat gradient for L1 (Fig. 7D,E versus Fig. 8D,E), while L3 did not show higher speed in the heat gradient (Fig. 7D,E versus Fig. 8D,E).

L1 were also much more likely to be observed in a bent body posture than L3 in the heat gradient (Fig. 8F); for example, L1 were found to be bent by 30 deg or more in about 25% of frames, while for L3 this was the case for only about 7% of all frames. Also, turn rate was much higher in L1 than in L3 (Fig. 8G). In effect, L1 gained less relative distance from their site of origin than L3 (Fig. 8H). While in principle this matches what was observed under free-crawling conditions (Fig. 7F–H), we note that the distance to origin that the animals gained per second was enhanced during thermotaxis, in particular for L1 but also for L3 (Fig. 7H versus Fig. 8H).

Thus, within a heat gradient, behaviour is obviously oriented for both L1 and L3. L1 appear more sensitive to the heat as the heat-induced modulation of speed and the heat-related gains in distance from origin appear more prominent.

Video tracking of light avoidance

When encountering a dark–light border zone, L1 and L3 showed avoidance behaviour at strikingly different probabilities. That is, 56.7% of such encounters resulted in retraction for L1 (212/374 encounters; Fig. S5B,C and Movie 6), while for L3 this was observed for only 31.3% of cases (167/534 encounters; Fig. S5B,C and Movie 6). This suggests that L1 are more light averse than L3.

Video tracking of chemotaxis

When located close to an odour source, both L1 and L3 remained in the vicinity of that odour source, resulting in 'ball-of-wool' trajectories (Fig. 9A,A′) not seen in the absence of odour (Fig. 9A″). We described tracks as sequences of runs and turns (Fig. 9B–B″). Mapping these tracks onto the respective reconstructed olfactory experience suggested that turns typically took place after the larvae moved down the odour gradient for some time, and that after a turn they moved up the odour gradient (Fig. 9C,C′). In other words, turns reoriented the larva up the odour gradient and thus eventually towards the odour source (behaviour in the absence of odour, i.e. in a 'fictive' odour gradient from a 'fictive' odour source located at a corresponding point in the arena, was confirmed to be random in this respect: Fig. 9C″). Indeed, the average olfactory experience during the 15 s preceding a turn consisted of negative changes in odour concentration; under such conditions, head casts towards the odour entailed a large and sudden rise in odour concentration such that this new direction was accepted and a turn was implemented (Fig. 9D,D′). Thus, turning manoeuvres resulted in a positive change in stimulus intensity in both L1 and L3. This was confirmed to not be the case for turns in the no-odour condition relative to a fictive odour source (Fig. 9D″), although turning manoeuvres with similar kinematics did take place under such conditions, too (see below). Specifically, in the presence of an odour source, L1 turned towards the local odour gradient in 79.4% of cases (114 turns towards the odour source of 29 larvae),

Journal of Experimental Biology (2017) 220, 2452-2475 doi:10.1242/jeb.156646

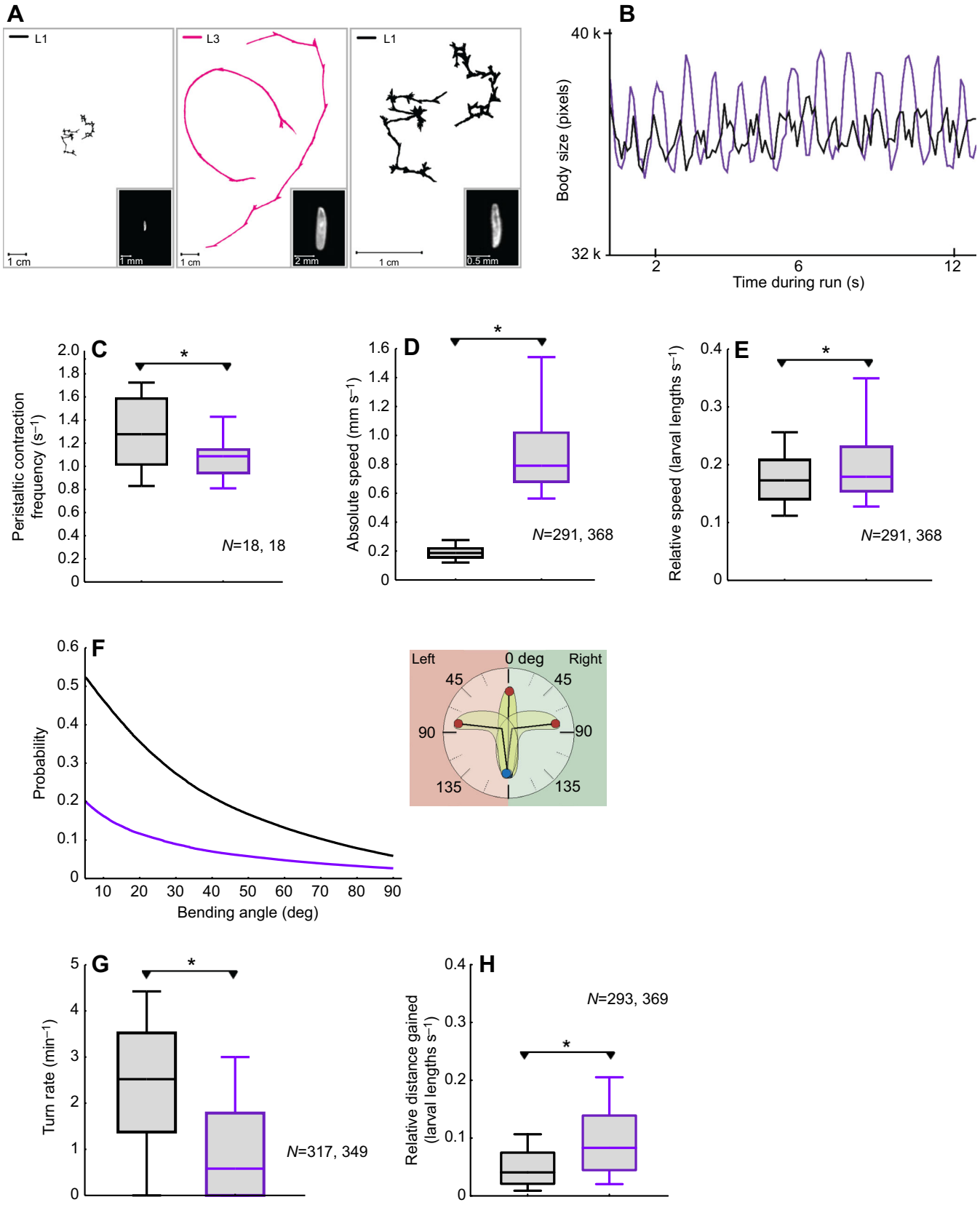

Fig. 7. See next page for legend.

Fig. 7. Video tracking of 'free' locomotion. (A) Examples of tracks of individual larvae from FIMTrack. Tracks of two L1 (black) and two L3 (magenta) under free-crawling conditions. Images of L1 are scaled to present them at the same absolute size (left) or at the same relative size (right) as L3 (middle). (B–E) Characterization of go-phases. B shows example plots of body size over time, indicating peristaltic contractions during a go-phase for L1 (black) and L3 (magenta). Note the slightly less regular organization of peristalsis in L1 compared with L3 (see also Movie 2). C gives the frequency of peristaltic contractions during go-phases, derived from the temporal maxima in body size of L1 (black box plots) and L3 (magenta box plots). Peristaltic contraction frequency is higher in L1 than in L3. D and E, respectively, show absolute and relative speed during go-phases in L1 (black box plots) and L3 (magenta box plots). Absolute speed is much lower in L1 than in L3. This difference is strongly reduced when considering speed relative to body length. *P<0.05 in MWU comparisons between L1 and L3. (F–H) Characterization of bending, turns and 'exploration range'. F shows the probability distribution of frames with bending angles ≥5 deg for L1 (black line) and L3 (magenta line). In L1, the likelihood of observing animals in a bent state was higher than in L3 for all considered bending angles. G shows turn rate of L1 (black box plots) is substantially higher than that of L3 (magenta box plots). H shows the gain in their relative distance to origin is less in L1 than in L3. This suggests a smaller exploration range in L1 than in L3, even when considered relative to body length. *P<0.05 in MWU comparisons between L1 and L3. Sample sizes are given within the figure.

while in the absence of a real odour source, the larvae implemented the expected approximately 50% of their turns towards a fictive odour source (85 turns towards a fictive odour source of 20 larvae; P<0.005, two-tailed t-test, data not shown). Parametrically, and as found in previous work on L3 (Gomez-Marin et al., 2011), the probability at which larvae of either stage turned towards the left side was highest whenever the odour gradient was pointing up to their left (i.e. at bearings close to 90 deg: Fig. 9E,E′) and lowest whenever the odour gradient was pointing up to their right (i.e. at bearings close to −90 deg: Fig. 9E,E′). This was not observed in the absence of odour relative to a fictive odour source (Fig. 9E″).

As for the kinematics of the turns, both L1 and L3 showed a reduced forward-speed of centroid movement immediately before a turn (Fig. 9F,F′); as expected from the smaller size of L1, this deceleration was less in L1 than in L3. Both L1 and L3 then initiated a head cast, characterized by a sharp increase of head-speed caused by lateral movement of the head (Fig. 9F,F′). The same kinematics of turning were observed for turns performed in the absence of odour (Fig. 9F″).

In addition to the turns analysed above, chemotaxis in L3 was reported to involve continuous slight bending of runs towards the local odour gradient – a process termed weathervaning (Gomez-Marin and Louis, 2014). We found that L1 also bias their runs in this way. Specifically, we observed a correlation between the instantaneous reorientation rate during runs versus the bearing angle between the direction of motion and the direction of the odour source (Fig. 9G,G′); as expected, no such relationship was observed in the absence of odour relative to a fictive odour source (Fig. 9G″). We note a trend in the weathervaning without an odour source, such that the larvae tended to bias their runs towards their right. This may hint at a handedness of larval turning behaviour in L1. Indeed, a weak trend suggesting such right-handedness was previously observed in L3 too (Gomez-Marin and Louis, 2014; see their fig. 1D).

DISCUSSION

In a community approach featuring 15 types of behavioural experiment, comprising contributions from 37 scientists in 12 labs, we have probed L1 *Drosophila* for various behavioural faculties that had previously been described for L3. With few exceptions, our results suggest qualitative concordance of behaviour in L1 and L3.

Before going into detail, we would like to stress that this suggestion of concordance is based on a lack of evidence for qualitative differences in behaviour between L1 and L3. This must not be confused with evidence for the absence of such differences. Indeed future studies using other or refined methods may well uncover qualitative differences in behaviour between L1 and L3. Still, the fact that across most of the presently used assays no such differences were uncovered does suggest some stability of behavioural organization across larval stages. Is this surprising?

During the 5–7 days between larval hatching and pupariation, larval *Drosophila* increase by approximately 60-fold in mass (considering approximated body proportions of 1 mm×0.25 mm ×0.25 mm=0.0625 mm^3 in L1 and 4 mm×1 mm×1 mm=4 mm^3 in L3). If a similar mass increase of 60-fold per week occurred in humans, assuming a birth weight of 3.5 kg, parents would face a gargantuan 210 kg baby after the first post-partum week. In other words, finding food and feeding are important to a larva, and will have evolutionarily shaped the organization of its behaviour and body plan. Indeed, the larval nervous system is considerably smaller than its salivary glands (Fig. 10A). The larval nervous system as established upon hatching thus must be immediately 'ready for life' not only in supporting an immediate competitive feeding frenzy but also to cope with a massively growing body. For the most part, this seems to be accomplished by the growth of neurons. At only some sites of the brain, such as the antennal lobe and most drastically the mushroom body (Ito and Hotta, 1992), it has been observed that further neurons continue to be knitted into the circuit and become functional during larval life. Furthermore, in Fig. 10B, examples of stable as well as dynamic transgene expression across larval stages are presented, speaking to both the stability and dynamics of gene regulation as related to the employed driver elements. Based on our present results, and we think surprisingly, the changes in body size and in the size and number of neurons seem largely inconsequential for larval behaviour – with the only apparent exceptions pertaining to the speed of locomotion, and salt- and light-related behaviour. These exceptional cases of discordance are discussed below in relation to their possible neurogenetic bases (regarding the cases of concordance between L1 and L3 behaviour, we refer the reader to the references cited in the Introduction and Results).

Speed of locomotion

L1 are about 4-fold slower in absolute speed than L3 (Figs 7D and 9F,F′; Fig. S4A). Behavioural measures of L1 not taking into account their slow speed may therefore yield systematically lower scores. This can be remedied by normalizing the data to speed, by using a scaled-down experimental set-up and/or by using paradigms that allow sufficient time until scores are taken.

We note that maintaining accuracy in behaviour at higher speed in L3 demands a better signal to noise ratio in neuronal processing, and that this may be one of the reasons why functionally redundant larval-born neurons are knitted into the embryonic-born circuits (see 'Brain organization: the mushroom bodies as an exceptional case', below). The same applies for the larva-to-adult transition.

Salt-related behaviour

L1 appear more sensitive to salt than L3, in a way that cannot be explained by differences in the speed of locomotion. This is the case for innate gustatory preference behaviour towards salt (Fig. 2F,G; Fig. S1) and for the effects of salt as a reinforcer (Fig. 3D,E) (also see Niewalda et al., 2008; Russell et al., 2011). That is, avoidance of and aversive learning about salt observed for L3 are seen earlier

Journal of Experimental Biology (2017) 220, 2452-2475 doi:10.1242/jeb.156646

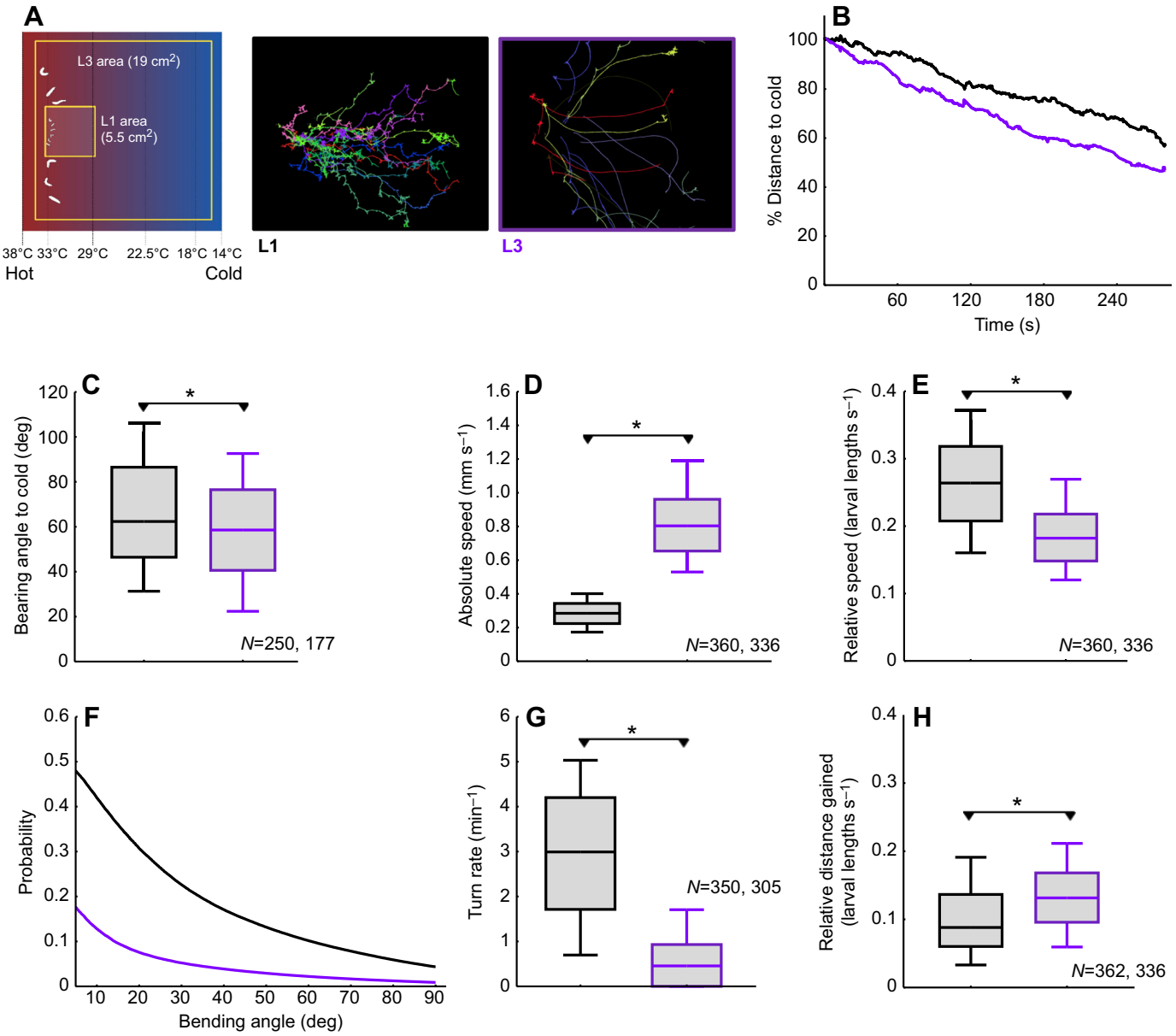

Fig. 8. Video tracking of thermotaxis. (A) Sketch of the thermotaxis set-up (left). Note that the area for L3 is 4-fold larger than that for L1, corresponding to the 4-fold difference in body length between L1 and L3. The heat gradient is linear; the covered temperatures are aversive for the respective stages within the observation areas delineated for L1 and L3. The two rightmost panels show screen shots of the final frames of Movie 5 with tracks of L1 and L3. Dimensions were normalized to body length. (B) Median distance to the cold side over time, with the distance at the origin of the tracks defined as 100% for both L1 (black line) and L3 (magenta line). (C–E) Characterization of go-phases in a linear heat gradient. C shows bearing angle to the cold side of L1 (black line) and L3 (magenta line). D and E, respectively, show absolute and relative speed during go-phases in L1 (black box plots) and L3 (magenta box plots). Absolute speed is much less in L1 than in L3. This difference is reversed when considering speed relative to body length. *P<0.05 in MWU comparisons between L1 and L3. (F–H) Characterization of bending, turns and 'exploration range' in a linear heat gradient. F shows probability distribution of frames with bending angles ≥5 deg for L1 (black line) and L3 (magenta line). In L1, the likelihood of observing animals in a bent state was higher than in L3 for all considered bending angles. G shows turn rate of L1 (black box plots) is substantially higher than that of L3 (magenta box plots). H shows the relative distance to origin is less in L1 than in L3. This suggests a smaller 'exploration range' in L1 than in L3, even when considered relative to body length. *P<0.05 in MWU comparisons between L1 and L3. Sample sizes are given within the figure.

during the experiment, are stronger and/or are observed at lower concentrations in L1. This higher sensitivity to salt may partially be caused by an unfavourable surface to volume ratio in L1, leading to higher sensitivity to desiccation stress. Also, the cuticle of L1 is softer than that of L3. Thus, micro-lesions of the cuticle caused by handling will be more likely and in combination with a possible irritation upon salt application will be of more impact for L1 than for L3. Furthermore, developmental differences in the expression of salt sensors and/or in the wiring of salt-sensitive sensory neurons and their downstream circuits may exist.

Light-related behaviour

The present data suggest that L1 are more light averse than L3. That is, in the employed light–annulus assay, the likelihood of a retraction response when encountering a dark–light border is almost twice as high for L1 as for L3 (Fig. S5B,C). Interestingly, the

Journal of Experimental Biology

Journal of Experimental Biology (2017) 220, 2452-2475 doi:10.1242/jeb.156646

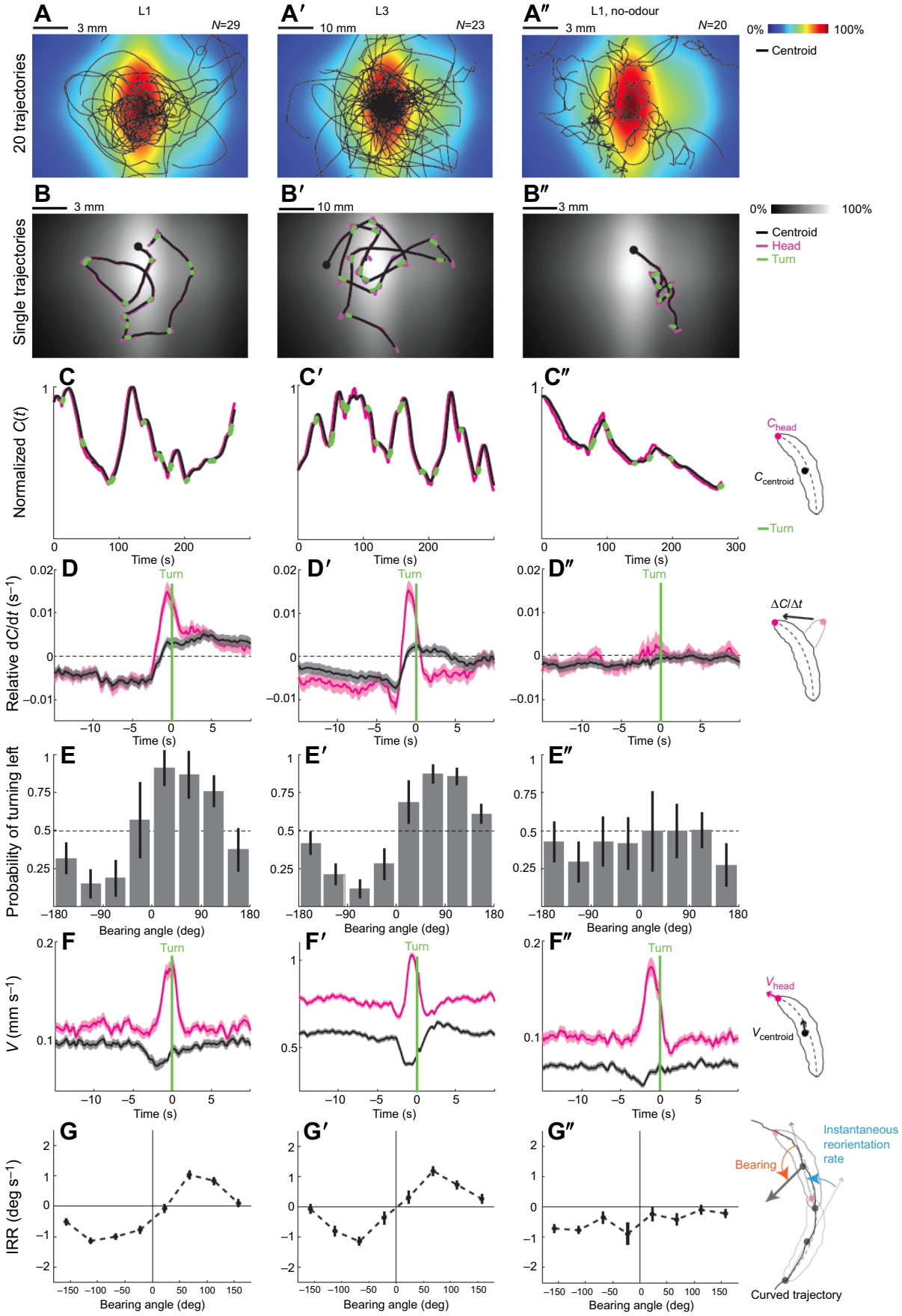

Fig. 9. See next page for legend.

Journal of Experimental Biology

Fig. 9. Video tracking of chemotaxis. (A–A″) Example tracks, based on centroid positions, for L1 (A) and L3 (A′) in a reconstructed odour gradient visualized by the colour scale. A″ shows tracks of L1 in the absence of odour, i.e. in this case the colour code indicates a 'fictive' odour landscape. (B–B″) Example trajectories of individual larvae in the three experimental conditions. The starting positions are marked with a black dot. The trajectory of the centroid is shown in black; the trajectory of the head is shown in magenta. Positions corresponding to turns are marked in green. (C–C″) Time courses of concentrations [normalized concentration, $C(t)$] corresponding to the example trajectories shown in B–B″. Turning manoeuvres are typically implemented after a prolonged period of moving down the odour gradient, in both L1 and L3 (C,C′). In the absence of odour, no such relationship is observed relative to a fictive odour source (C″). (D–D″) Turn-triggered averages of the relative changes in odour concentration (dC/dt) at the centroid (black) and at the head (magenta). When moving down-gradient, the beginning of the turning manoeuvre in both L1 and L3 is associated with a sharp rise in odour concentration at the head, corresponding to a head cast towards the odour source. This entails acceptance of the new direction and completion of the turning manoeuvre (D,D′). Note that turning manoeuvres in the absence of an odour (F″) do not show these features relative to a fictive odour source (D″). (E–E″) Within an odour gradient, turns are more likely to take place towards rather than away from the odour, in both L1 and L3 (E,E′). According to the convention used, for positive bearings, left turns reorient the larva up the odour gradient, i.e. effectively towards the odour source. Such turns were most likely for bearing angles around 90 deg; that is, when the larvae were oriented perpendicularly to the odour gradient. For negative bearings, turns towards the right reorient the larvae up the odour gradient; these are most frequent at −90 deg. In the absence of odour, no such relationship is observed relative to a fictive odour source (E″). Error bars represent an estimate of the standard error calculated based on a bootstrap procedure. (F–F″) Turn-triggered averages of head speed (magenta) and centroid speed (black) during turning manoeuvres. Before a turn, centroid speed declines, while head speed increases. This is the case for both L1 and L3 navigating in an odour gradient (F,F′), and is also true for turning manoeuvres in the absence of odour (F″). Error bars show the confidence interval (5th to 95th percentile). Note the approximately 5-fold higher speed in L1 (F,F″) than in L3 (F′). (G–G″) Trajectories during run periods in an odour gradient are often bent up the odour gradient, i.e. towards the odour source (A,A′). To quantify the underlying behaviour, weathervaning was measured as the relationship between the average instantaneous reorientation rate (IRR) and the local bearing angle. This shows that both L1 and L3 bent their runs most strongly toward the odour source when oriented perpendicularly to it, i.e. at bearings of ±90 deg. The grey arrow indicates the direction of the odour gradient. Error bars show the confidence interval (5th to 95th percentile). Sample sizes are given within the figure.

preference scores from a light–dark quadrant assay measured after light–electroshock training are not apparently more negative for L1 than for L3 (Fig. 5B) (Sawin-MacCormack et al., 1995). This could imply that in assays of that type, more time needs to be allowed for L1 to reveal the full extent of their light avoidance and/or of light–electroshock associative memory. In other words, what appears to be an inability to form light–electric shock associations in L1 may partially reflect that assay conditions are suboptimal for L1, revealing only a weak trend for aversive memory (Fig. 5). Data on the behaviour of L1 in a light gradient are not yet available.

Considering that in addition to suboptimal assay conditions there may be 'true' biological reasons for the poor light–electroshock association scores in L1, we note that L1 are capable of learning with electroshock as punishment if odours are used for association (Aceves-Piña and Quinn, 1979). This implies that it may be visual processing, rather than electric shock processing, that is not permissive for association formation. In this context, it seems relevant that serotonergic neurons innervating the larval optic neuropil start to form extensive ramifications only in late, wandering L3 (Mukhopadhyay and Campos, 1995); this innervation has previously been related to the loss of light avoidance upon the transition from feeding L3 to wandering L3 (Sawin-MacCormack et al., 1995). Also, the larval mushroom body lacks serotonergic innervation (Blenau and Thamm, 2011; Giang et al., 2011; Huser et al., 2012); specifically, the serotonergic CSD neuron is present in larvae, yet innervates the mushroom bodies only after metamorphosis (Huser et al., 2012; Roy et al., 2007). It is therefore tempting to speculate that alterations in serotonergic signalling may be partially responsible for differences in light aversion and/or light–electroshock associative learning across larval stages, in particular as pupariation approaches. Changes in serotonergic signalling may also impact other behavioural alterations along the larval–pupal transition, such as changes in geotaxis, aggregation and locomotion.

Brain organization: the mushroom bodies as an exceptional case

To date, surprisingly few discrepancies have been revealed between an L1 nervous system reconstructed at synaptic resolution from the electron microscope versus what was known before from studies based on light microscopy. Arguably, the most significant of these discrepancies, in addition to what has been mentioned above regarding the serotonin system, relates to the mushroom body, a higher-order brain centre of insects required for learning and memory (Heisenberg, 2003). That is, the number of mushroom body-intrinsic Kenyon cells (KCs) increases from about 100 in L1 (Eichler et al., 2017) to 800–1200 in L3 (Ito and Hotta, 1992). In no other case have similarly massive increases in neuron number during larval stages been reported. If the added KCs were simply redundant to the already existing ones, one may interpret this as reflecting the need for a better signal to noise ratio in L3 because of their higher speed of locomotion. Interestingly, however, a group of about 20 early-born KCs qualitatively differs from the later-born ones in their connectivity to the second-order sensory projection neurons (PNs) that map sensory information onto the KCs (Eichler et al., 2017). That is, each early-born KC has just one claw, a postsynaptic specialization by which it connects to just one PN. In turn, PNs connect to just one such early-born KC, plus, later on, a random set of about 4–8 later-born KCs. These later-born KCs typically sample 2–6 PNs. Thus, for the earliest set of PN–KC connections, a 1:1 connectivity makes sure that all PNs get fairly sampled. Once this is achieved, combinatorial and randomized PN–KC connections are added to fine-tune the sensory representation across the KCs. This implies that mushroom body function in L1 is more narrowly constrained by a 1:1 PN–KC connectivity than is the case in L3. As far as associative olfactory learning abilities are concerned, this does not seem to lead to qualitative differences in mnemonic ability between L1 and L3 (Fig. 3) (Aceves-Piña and Quinn, 1979; Heisenberg et al., 1985; Scherer et al., 2003; Neuser et al., 2005; Niewalda et al., 2008; Gerber and Hendel, 2006; Pauls et al., 2010; El-Keredy et al., 2012; Schleyer et al., 2015a). Clearly, however, differences in, for example, the stimulus-specificity of memory, in the ability to detect components from compound stimuli or the ability to discern stimuli from contextual background may be expected.

Taken together, despite massive growth, there appears to be a phase of relative stability in brain organization between L1 and L3. Clearly, however, profound reorganization then takes place during the pupal stages and into early adulthood (Levine et al., 1995; Truman, 1996; Consoulas et al., 2000; Tissot and Stocker, 2000). As discussed above for the visual system as an example, much of this is indeed foreshadowed at the end of larval life, as larvae develop out of feeding L3 and into wandering L3 and pupae. These changes in behavioural and brain organization during the larval–pupal transition may warrant a separate survey.

In conclusion, our results show a striking match in the behavioural faculties of L1 and L3. Keeping due caveats in mind,

Journal of Experimental Biology (2017) 220, 2452-2475 doi:10.1242/jeb.156646

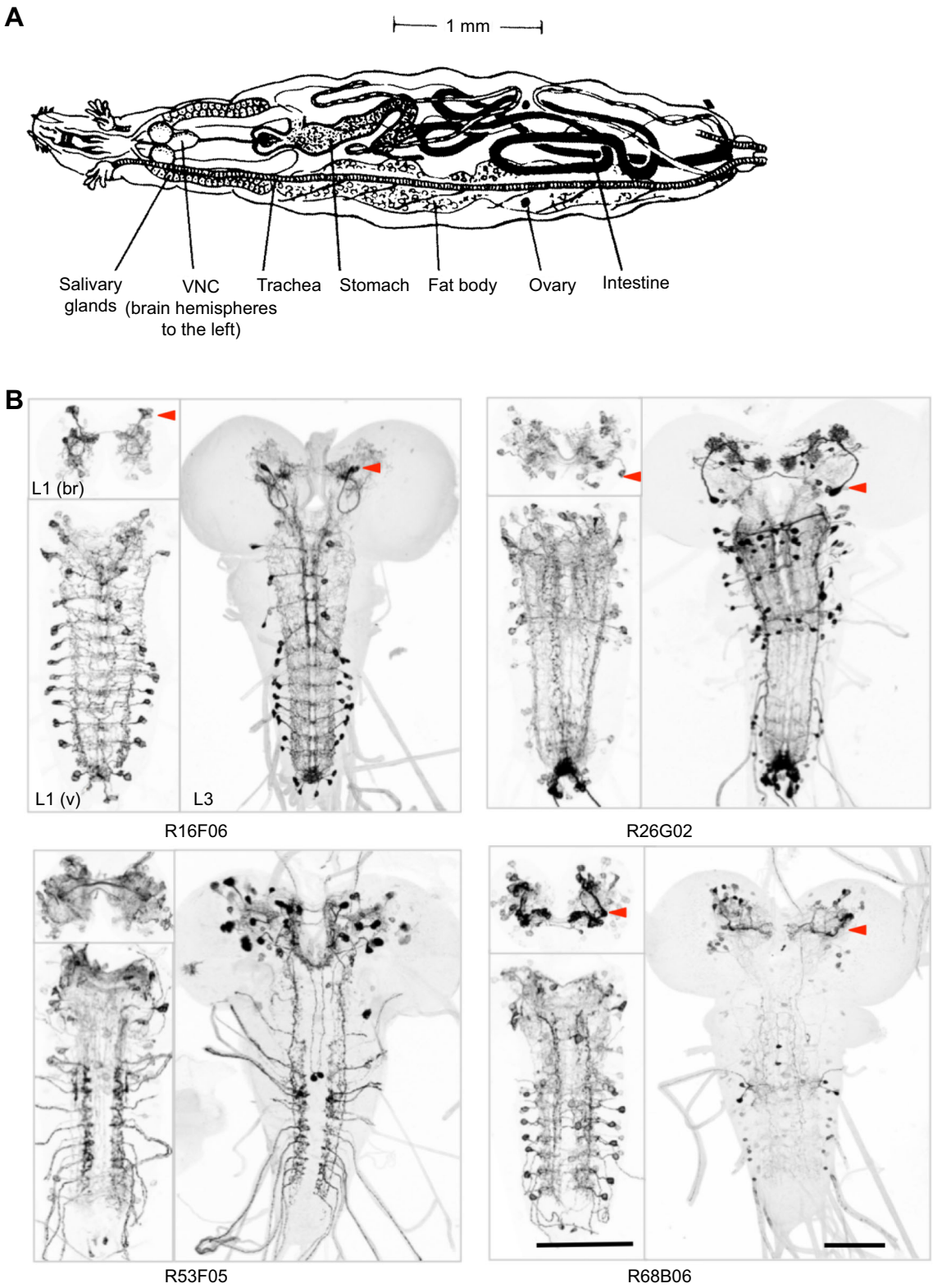

Fig. 10. Stability and dynamics of transgene expression across larval stages. (A) Schematic overview of the body plan and internal organs of an L3 (modified from Demerec and Kaufmann, 1972; image courtesy of The Carnegie Institution). (B) Confocal projections of L1 and L3 nervous systems for four different driver strains of the Janelia collection (Li et al., 2014). For L1, separate projections are provided for the brain (br) and the ventral nervous system (v). The chosen strains maintain expression, visualized via anti-GFP staining of brains from crosses of the indicated driver strains with UAS-GFP, in many of the same neurons throughout larval stages. R16F06 shows expression in the AVM011 interneurons of the brain (arrowhead) and in two pairs of segmentally repeated interneurons. R26G02 shows expression in the APL neuron (arrowhead) that innervates the mushroom bodies. R53F05 expresses in a variety of brain interneurons and segmental sensory neurons, and R68B06 expresses in embryonic-born Kenyon cells of the mushroom bodies (arrowhead). In the latter line, expression in the segmental interneurons is largely lost before stage 3 is reached. In other cases, additional expression may be seen in stage 3 (not shown). Indeed, expression patterns often are dynamic across larval stages (Li et al., 2014), such that they must be ascertained on a case-by-case basis. The scale bar represents 100 µm.

Journal of Experimental Biology

it thus appears valid to interpret the behavioural faculties of L3 in the context of the electron microscope-based synaptic connectome described for L1, and vice versa.

Acknowledgements
We thank J. Herrmann for help with the FIM set-up (Münster), H. Reim, C. Tauber, J. Saumweber and B. Kracht for laboratory assistance (Magdeburg), Aljoscha Nern and Gerald Rubin (Janelia) for kindly providing the UAS-HA stock, and R. Glasgow, Zaragoza, Spain, for language editing.

Competing interests
The authors declare no competing or financial interests.

Author contributions
Conceptualization: B.G., C. Klaembt, M.J.P., A.S.T.; Formal analysis: M.J.A.-C., D.B., A.B., Y.C., K.E., C.E., P.M.F., B.G., N.H., X.J., J.K., C. Klaembt, C. Koenig, M.L., B.M., A.M., C.M., D.M., T.N., N.O., E.P., M.J.P., M.P., N. Ramsperger, N. Randel, B.R., T.S., P. Schlegel, M.S., P. Soba, S.G.S., T.T., N.T., J.W.T., A.Y., M.Z.; Investigation: M.J.A.-C., D.B., A.B., Y.C., K.E., C.E., P.M.F., N.H., X.J., J.K., C. Koenig, M.L., B.M., A.M., C.M., D.M., N.O., E.P., M.P., N. Ramsperger, N. Randel, B.R., T.S., P. Schlegel, M.S., P. Soba, S.G.S., T.T., N.T., J.W.T., A.Y., M.Z.; Writing - original draft: Y.C., B.G., T.N. Writing - review & editing: M.J.A.-C., D.B., A.B., Y.C., K.E., C.E., P.M.F., B.G., N.H., X.J., J.K., C. Klaembt, C. Koenig, M.L., B.M., A.M., C.M., D.M., T.N., N.O., E.P., M.J.P., M.P., N. Ramsperger, N. Randel, B.R., T.S., P. Schlegel, M.S., P. Soba, S.G.S., T.T., A.S.T., N.T., J.W.T., A.Y., M.Z.; Project administration: Y.C., B.G., C. Klaembt, T.N., M.J.P., A.S.T.

Funding
The Gulbenkian/Melbourne group was supported by the Fundação para a Ciência e a Tecnologia (FCT; post-doctoral fellowship to M.J.A.-C.: SFRH/BPD/75993/2011; exploratory grant to M.J.A.-C. and C.K.M.: EXPL/BEX-BID/0497/2013). The Münster group was supported by the Cluster of Excellence Cells in Motion (CiM) and the CiM International Max Planck research school (CiM-IMPRS). The Barcelona group was supported by the Spanish Ministry of Economy and Competitiveness, 'Centro de Excelencia Severo Ochoa 2013-2017' (SEV-2012-0208), the CERCA Programme/Generalitat de Catalunya, the 'la Caixa' International PhD Programme, and the Spanish Ministry of Science and Innovation (BFU2011-26208). The LIN-GoLM group received support from the Wissenschaftsgemeinschaft Gottfried Wilhelm Leibniz, the State of Sachsen-Anhalt, the Center for Behavioral Brain Sciences Magdeburg and the Otto von Guericke Universität Magdeburg, as well as from the Deutsche Forschungsgemeinschaft (CRC 779 Motivated behaviour: B11; GE1091/4-1) and the European Commission (FP7-ICT project Miniature Insect Model for Active Learning MINIMAL). The Janelia group received support from the Howard Hughes Medical Institute. The Fribourg group was supported by a starter grant from the European Research Council (ERC-2012-StG 309832-PhotoNaviNet) and the Swiss National Science Foundation (31003A_169993). The Hamburg group was supported by the Deutsche Forschungsgemeinschaft (SPP 1926, Next generation optogenetics, SO1337/2-1), and the Landesforschungsförderung Hamburg (LFF-FV27). The LIN-MolSysBiol group received support from the Wissenschaftsgemeinschaft Gottfried Wilhelm Leibniz, the State of Sachsen-Anhalt, the Center for Behavioral Brain Sciences Magdeburg and the Deutsche Forschungsgemeinschaft (CRC 779 Motivated behaviour: B15; YA272/2-1). The Bonn group was supported by the Deutsche Forschungsgemeinschaft (PA 787/7-1) and Cluster of Excellence ImmunoSensation. The Konstanz group was supported by Deutsche Forschungsgemeinschaft (TH1584/1-1, TH1584/3-1), the Baden-Württemberg Stiftung and the Zukunftskolleg of the University of Konstanz.

Supplementary information
Supplementary information available online at
http://jeb.biologists.org/lookup/doi/10.1242/jeb.156646.supplemental

References

Aceves-Piña, E. O. and Quinn, W. G. (1979). Learning in normal and mutant Drosophila larvae. *Science* **206**, 93-96.
Apostolopoulou, A. A., Widmann, A., Rohwedder, A., Pfitzenmaier, J. E. and Thum, A. S. (2013). Appetitive associative olfactory learning in Drosophila larvae. *J. Vis. Exp.* e4334.
Benzer, S. (1967). Behavioral mutants of Drosophila isolated by countercurrent distribution. *Proc. Natl. Acad. Sci. USA* **58**, 1112-1119.
Berck, M. E., Khandelwal, A., Claus, L., Hernandez-Nunez, L., Si, G., Tabone, C. J., Li, F., Truman, J. W., Fetter, R. D., Louis, M. et al. (2016). The wiring diagram of a glomerular olfactory system. *Elife* **5**, e14859.
Bjordal, M., Arquier, N., Kniazeff, J., Pin, J. P. and Léopold, P. (2014). Sensing of amino acids in a dopaminergic circuitry promotes rejection of an incomplete diet in Drosophila. *Cell* **156**, 510-521.
Blenau, W. and Thamm, M. (2011). Distribution of serotonin (5-HT) and its receptors in the insect brain with focus on the mushroom bodies: lessons from Drosophila melanogaster and Apis mellifera. *Arthropod. Struct. Dev.* **40**, 381-394.
Brand, A. H. and Perrimon, N. (1993). Targeted gene expression as a means of altering cell fates and generating dominant phenotypes. *Development* **118**, 401-415.
Cobb, M. (1999). What and how do maggots smell? *Biol. Rev.* **74**, 425-459.
Consoulas, C., Duch, C., Bayline, R. J. and Levine, R. B. (2000). Behavioral transformations during metamorphosis: remodeling of neural and motor systems. *Brain Res. Bull.* **53**, 571-583.
Croset, V., Schleyer, M., Arguello, J. R., Gerber, B. and Benton, R. (2016). A molecular and neuronal basis for amino acid sensing in the Drosophila larva. *Sci. Rep.* **6**, 34871.
Demerec, M. and Kaufmann, B. P. (1972). *Drosophila Guide. Introduction to the Genetics and Cytology of Drosophila melanogaster*. Washington, DC: The Carnegie Institution.
Diegelmann, S., Klagges, B., Michels, B., Schleyer, M. and Gerber, B. (2013). Maggot learning and Synapsin function. *J. Exp. Biol.* **216**, 939-951.
Dudai, Y., Jan, Y. N., Byers, D., Quinn, W. G. and Benzer, S. (1976). Dunce, a mutant of Drosophila deficient in learning. *Proc. Natl. Acad. Sci. USA* **73**, 1684-1688.
Eichler, K., Li, F., Litwin-Kumar, A., Park, Y., Andrade, I., Schneider-Mizell, C. M., Saumweber, T., Huser, A., Bonnery, D., Gerber, B. et al. (2017). The complete wiring diagram of a high-order learning and memory center, the insect mushroom body. *Nature* (in press).
El-Keredy, A., Schleyer, M., König, C., Ekim, A. and Gerber, B. (2012). Behavioural analyses of quinine processing in choice, feeding and learning of larval Drosophila. *PLoS ONE* **7**, e40525.
Eschbach, C., Cano, C., Haberkern, H., Schraut, K., Guan, C., Triphan, T. and Gerber, B. (2011). Associative learning between odorants and mechanosensory punishment in larval Drosophila. *J. Exp. Biol.* **214**, 3897-3905.
Frye, M. A. and Dickinson, M. H. (2004). Closing the loop between neurobiology and flight behavior in Drosophila. *Curr. Opin. Neurobiol.* **14**, 729-736.
Fushiki, A., Zwart, M. F., Kohsaka, H., Fetter, R. D., Cardona, A. and Nose, A. (2016). A circuit mechanism for the propagation of waves of muscle contraction in Drosophila. *Elife* **5**, e13253.
Garrity, P. A., Goodman, M. B., Samuel, A. D. and Sengupta, P. (2010). Running hot and cold: behavioral strategies, neural circuits, and the molecular machinery for thermotaxis in C. elegans and Drosophila. *Genes Dev.* **24**, 2365-2382.
Gasque, G., Conway, S., Huang, J., Rao, Y. and Vosshall, L. B. (2013). Small molecule drug screening in Drosophila identifies the 5HT2A receptor as a feeding modulation target. *Sci. Rep.* **3**, srep02120.
Gerber, B. and Hendel, T. (2006). Outcome expectations drive learned behaviour in larval Drosophila. *Proc. Biol. Sci.* **273**, 2965-2968.
Gerber, B. and Stocker, R. F. (2007). The Drosophila larva as a model for studying chemosensation and chemosensory learning: a review. *Chem. Senses* **32**, 65-89.
Gerber, B., Biernacki, R. and Thum, J. (2010). Odour-sugar learning in larval Drosophila. In *Drosophila Neurobiology Methods: A Laboratory Manual* (ed. B. Zhang, M. R. Freemann and S. Waddell), pp. 443-455. Cold Spring Harbor: CSHL Press.
Gerber, B., Biernacki, R. and Thum, J. (2013). Odor-taste learning assays in Drosophila larvae. *Cold Spring Harb. Protoc.* 213-223.
Giang, T., Ritze, Y., Rauchfuss, S., Ogueta, M. and Scholz, H. (2011). The serotonin transporter expression in Drosophila melanogaster. *J. Neurogenet.* **25**, 17-26.
Gomez-Marin, A. and Louis, M. (2012). Active sensation during orientation behavior in the Drosophila larva: more sense than luck. *Curr. Opin. Neurobiol.* **22**, 208-215.
Gomez-Marin, A. and Louis, M. (2014). Multilevel control of run orientation in Drosophila larval chemotaxis. *Front. Behav. Neurosci.* **8**, 38.
Gomez-Marin, A., Stephens, G. J. and Louis, M. (2011). Active sampling and decision making in Drosophila chemotaxis. *Nat. Commun.* **2**, 441.
Gomez-Marin, A., Partoune, N., Stephens, G. J. and Louis, M. (2012). Automated tracking of animal posture and movement during exploration and sensory orientation behaviors. *PLoS ONE* **7**, e41642.
Heisenberg, M. (2003). Mushroom body memoir: from maps to models. *Nat. Rev. Neurosci.* **4**, 266-275.
Heisenberg, M., Borst, A., Wagner, S. and Byers, D. (1985). Drosophila mushroom body mutants are deficient in olfactory learning. *J. Neurogenet.* **2**, 1-30.
Hotta, Y. and Benzer, S. (1970). Genetic dissection of the Drosophila nervous system by means of mosaics. *Proc. Natl. Acad. Sci. USA* **67**, 1156-1163.
Huser, A., Rohwedder, A., Apostolopoulou, A. A., Widmann, A., Pfitzenmaier, J. E., Maiolo, E. M., Selcho, M., Pauls, D., von Essen, A., Gupta, T. et al. (2012). The serotonergic central nervous system of the Drosophila larva: anatomy and behavioral function. *PLoS ONE* **7**, e47518.
Hwang, R. Y., Zhong, L., Xu, Y., Johnson, T., Zhang, F., Deisseroth, K. and Tracey, W. D. (2007). Nociceptive neurons protect Drosophila larvae from parasitoid wasps. *Curr. Biol.* **17**, 2105-2116.

Ito, K. and Hotta, Y. (1992). Proliferation pattern of postembryonic neuroblasts in the brain of Drosophila melanogaster. *Dev. Biol.* **149**, 134-148.
Jenett, A., Rubin, G. M., Ngo, T.-T. B., Shepherd, D., Murphy, C., Dionne, H., Pfeiffer, B. D., Cavallaro, A., Hall, D., Jeter, J. et al. (2012). A GAL4-driver line resource for Drosophila neurobiology. *Cell Rep.* **2**, 991-1001.
Johnston, D. S. and Nüsslein-Volhard, C. (1992). The origin of pattern and polarity in the Drosophila embryo. *Cell* **68**, 201-219.
Jovanic, T., Schneider-Mizell, C. M., Shao, M., Masson, J.-B., Denisov, G., Fetter, R. D., Mensh, B. D., Truman, J. W., Cardona, A. and Zlatic, M. (2016). Competitive disinhibition mediates behavioral choice and sequences in Drosophila. *Cell* **167**, 858-870.e19.
Kane, E. A., Gershow, M., Afonso, B., Larderet, I., Klein, M., Carter, A. R., de Bivort, B. L., Sprecher, S. G. and Samuel, A. D. T. (2013). Sensorimotor structure of Drosophila larva phototaxis. *Proc. Natl. Acad. Sci. USA* **110**, E3868-E3877.
Keene, A. C. and Sprecher, S. G. (2012). Seeing the light: photobehavior in fruit fly larvae. *Trends Neurosci.* **35**, 104-110.
Kernan, M., Cowan, D. and Zuker, C. (1994). Genetic dissection of mechanosensory transduction: mechanoreception-defective mutations of Drosophila. *Neuron* **12**, 1195-1206.
Klapoetke, N. C., Murata, Y., Kim, S. S., Pulver, S. R., Birdsey-Benson, A., Cho, Y. K., Morimoto, T. K., Chuong, A. S., Carpenter, E. J., Tian, Z. et al. (2014). Independent optical excitation of distinct neural populations. *Nat. Methods* **11**, 338-346.
Konopka, R. J. and Benzer, S. (1971). Clock mutants of Drosophila melanogaster. *Proc. Natl. Acad. Sci. USA* **68**, 2112-2116.
Kudow, N., Miura, D., Schleyer, M., Toshima, N., Gerber, B. and Tanimura, T. (2017). Preference for and learning of amino acids in larval Drosophila. *Biol. Open*. **6**, 365-369.
Levine, R. B., Morton, D. B. and Restifo, L. L. (1995). Remodeling of the insect nervous system. *Curr. Opin. Neurobiol.* **5**, 28-35.
Li, H.-H., Kroll, J. R., Lennox, S. M., Ogundeyi, O., Jeter, J., Depasquale, G. and Truman, J. W. (2014). A GAL4 driver resource for developmental and behavioral studies on the larval CNS of Drosophila. *Cell Rep.* **8**, 897-908.
Littleton, J. T. and Ganetzky, B. (2000). Ion channels and synaptic organization: analysis of the Drosophila genome. *Neuron* **26**, 35-43.
Liu, C., Plaçais, P.-Y., Yamagata, N., Pfeiffer, B. D., Aso, Y., Friedrich, A. B., Siwanowicz, I., Rubin, G. M., Preat, T. and Tanimoto, H. (2012). A subset of dopamine neurons signals reward for odour memory in Drosophila. *Nature* **488**, 512-516.
Louis, M., Huber, T., Benton, R., Sakmar, T. P. and Vosshall, L. B. (2008a). Bilateral olfactory sensory input enhances chemotaxis behavior. *Nat. Neurosci.* **11**, 187-199.
Louis, M., Piccinotti, S. and Vosshall, L. B. (2008b). High-resolution measurement of odor-driven behavior in Drosophila larvae. *J. Vis. Exp.* e638.
Martinez, W. L. and Martinez, A. R. (2012). *Computational Statistics Handbook with MATLAB*. London: CRC press.
Michels, B., Saumweber, T., Biernacki, R., Thum, J., Glasgow, R. D. V., Schleyer, M., Chen, Y.-C., Eschbach, C., Stocker, R. F., Toshima, N. et al. (2017). Pavlovian conditioning of larval Drosophila: An illustrated, multilingual, hands-on manual for odor-taste associative learning in maggots. *Front. Behav. Neurosci.* **11**, 45.
Mukhopadhyay, M. and Campos, A. R. (1995). The larval optic nerve is required for the development of an identified serotonergic arborization in Drosophila melanogaster. *Dev. Biol.* **169**, 629-643.
Neckameyer, W. S. (2010). A trophic role for serotonin in the development of a simple feeding circuit. *Dev. Neurosci.* **32**, 217-237.
Nern, A., Pfeiffer, B. D. and Rubin, G. M. (2015). Optimized tools for multicolor stochastic labeling reveal diverse stereotyped cell arrangements in the fly visual system. *Proc. Natl. Acad. Sci. USA* **112**, E2967-E2976.
Neuser, K., Husse, J., Stock, P. and Gerber, B. (2005). Appetitive olfactory learning in Drosophila larvae: effects of repetition, reward strength, age, gender, assay type and memory span. *Anim. Behav.* **69**, 891-898.
Niewalda, T., Singhal, N., Fiala, A., Saumweber, T., Wegener, S. and Gerber, B. (2008). Salt processing in larval Drosophila: choice, feeding, and learning shift from appetitive to aversive in a concentration-dependent way. *Chem. Senses* **33**, 685-692.
Ohyama, T., Jovanic, T., Denisov, G., Dang, T. C., Hoffmann, D., Kerr, R. A. and Zlatic, M. (2013). High-throughput analysis of stimulus-evoked behaviors in Drosophila larva reveals multiple modality-specific escape strategies. *PLoS ONE* **8**, e71706.
Ohyama, T., Schneider-Mizell, C. M., Fetter, R. D., Aleman, J. V., Franconville, R., Rivera-Alba, M., Mensh, B. D., Branson, K. M., Simpson, J. H., Truman, J. W. et al. (2015). A multilevel multimodal circuit enhances action selection in Drosophila. *Nature* **520**, 633-639.
O'Kane, C. J. and Gehring, W. J. (1987). Detection in situ of genomic regulatory elements in *Drosophila*. *Proc. Natl. Acad. Sci. USA* **84**, 9123-9127.
Otto, N., Risse, B., Berh, D., Bittern, J., Jiang, X. and Klämbt, C. (2016). Interactions among Drosophila larvae before and during collision. *Sci. Rep.* **6**, 31564.
Pauls, D., Selcho, M., Gendre, N., Stocker, R. F. and Thum, A. S. (2010). Drosophila larvae establish appetitive olfactory memories via mushroom body neurons of embryonic origin. *J. Neurosci.* **30**, 10655-10666.
Pfeiffer, B. D., Jenett, A., Hammonds, A. S., Ngo, T.-T. B., Misra, S., Murphy, C., Scully, A., Carlson, J. W., Wan, K. H., Laverty, T. R. et al. (2008). Tools for neuroanatomy and neurogenetics in Drosophila. *Proc. Natl. Acad. Sci. USA* **105**, 9715-9720.
Pfeiffer, B. D., Ngo, T.-T. B., Hibbard, K. L., Murphy, C., Jenett, A., Truman, J. W. and Rubin, G. M. (2010). Refinement of tools for targeted gene expression in Drosophila. *Genetics* **186**, 735-755.
R Core Team (2017). *R: A Language and Environment for Statistical Computing*. R Foundation for Statistical Computing, Vienna, Austria.
Risse, B., Thomas, S., Otto, N., Löpmeier, T., Valkov, D., Jiang, X. and Klämbt, C. (2013). FIM, a novel FTIR-based imaging method for high throughput locomotion analysis. *PLoS ONE* **8**, e53963.
Risse, B., Otto, N., Berh, D., Jiang, X. and Klämbt, C. (2014). FIM imaging and FIMtrack: two new tools allowing high-throughput and cost effective locomotion analysis. *J. Vis. Exp.*, e52207.
Rodrigues, V. (1980). Olfactory behavior of Drosophila melanogaster. *Basic Life Sci.* **16**, 361-371.
Rohwedder, A., Pfitzenmaier, J. E., Ramsperger, N., Apostolopoulou, A. A., Widmann, A. and Thum, A. S. (2012). Nutritional value-dependent and nutritional value-independent effects on Drosophila melanogaster larval behavior. *Chem. Senses* **37**, 711-721.
Rohwedder, A., Wenz, N. L., Stehle, B., Huser, A., Yamagata, N., Zlatic, M., Truman, J. W., Tanimoto, H., Saumweber, T., Gerber, B. et al. (2016). Four individually identified paired dopamine neurons signal reward in larval Drosophila. *Curr. Biol.* **26**, 661-669.
Roy, B., Singh, A. P., Shetty, C., Chaudhary, V., North, A., Landgraf, M., Vijayraghavan, K. and Rodrigues, V. (2007). Metamorphosis of an identified serotonergic neuron in the Drosophila olfactory system. *Neural Dev.* **2**, 20.
Rubin, G. M. and Spradling, A. C. (1982). Genetic transformation of Drosophila with transposable element vectors. *Science* **218**, 348-353.
Russell, C., Wessnitzer, J., Young, J. M., Armstrong, J. D. and Webb, B. (2011). Dietary salt levels affect salt preference and learning in larval Drosophila. *PLoS ONE* **6**, e20100.
Saumweber, T., Husse, J. and Gerber, B. (2011). Innate attractiveness and associative learnability of odors can be dissociated in larval Drosophila. *Chem. Senses* **36**, 223-235.
Saumweber, T., Cano, C., Klessen, J., Eichler, K., Fendt, M. and Gerber, B. (2014). Immediate and punitive impact of mechanosensory disturbance on olfactory behaviour of larval Drosophila. *Biol. Open* **3**, 1005-1010.
Sawin-McCormack, E. P., Sokolowski, M. B. and Campos, A. R. (1995). Characterization and genetic analysis of Drosophila melanogaster photobehavior during larval development. *J. Neurogenet.* **10**, 119-135.
Scherer, S., Stocker, R. F. and Gerber, B. (2003). Olfactory learning in individually assayed Drosophila larvae. *Learn. Mem.* **10**, 217-225.
Schipanski, A., Yarali, A., Niewalda, T. and Gerber, B. (2008). Behavioral analyses of sugar processing in choice, feeding, and learning in larval Drosophila. *Chem. Senses* **33**, 563-573.
Schlegel, P., Texada, M. J., Miroschnikow, A., Schoofs, A., Huckesfeld, S., Peters, M., Schneider-Mizell, C. M., Lacin, H., Li, F., Fetter, R. D. et al. (2016). Synaptic transmission parallels neuromodulation in a central food-intake circuit. *Elife* **5**, e16799.
Schleyer, M., Saumweber, T., Nahrendorf, W., Fischer, B., von Alpen, D., Pauls, D., Thum, A. and Gerber, B. (2011). A behavior-based circuit model of how outcome expectations organize learned behavior in larval Drosophila. *Learn. Mem.* **18**, 639-653.
Schleyer, M., Diegelmann, S., Michels, B., Saumweber, T. and Gerber, B. (2013). 'Decision making' in larval Drosophila. In *Invertebrate Learning and Memory* (ed. R. Menzel and P. Benjamin), pp. 41-55. Amsterdam: Elsevier.
Schleyer, M., Miura, D., Tanimura, T. and Gerber, B. (2015a). Learning the specific quality of taste reinforcement in larval Drosophila. *Elife* **4**, e04711.
Schleyer, M., Reid, S. F., Pamir, E., Saumweber, T., Paisios, E., Davies, A., Gerber, B. and Louis, M. (2015b). The impact of odor-reward memory on chemotaxis in larval Drosophila. *Learn. Mem.* **22**, 267-277.
Schneider-Mizell, C. M., Gerhard, S., Longair, M., Kazimiers, T., Li, F., Zwart, M. F., Champion, A., Midgley, F. M., Fetter, R. D., Saalfeld, S. et al. (2016). Quantitative neuroanatomy for connectomics in Drosophila. *Elife* **5**, e12059.
Schoofs, A., Hückesfeld, S., Schlegel, P., Miroschnikow, A., Peters, M., Zeymer, M., Spieß, R., Chiang, A.-S. and Pankratz, M. J. (2014). Selection of motor programs for suppressing food intake and inducing locomotion in the Drosophila brain. *PLoS Biol.* **12**, e1001893.
Sivanantharajah, L. and Zhang, B. (2015). Current techniques for high-resolution mapping of behavioral circuits in Drosophila. *J. Comp. Physiol. A Neuroethol. Sens. Neural Behav. Physiol.* **201**, 895-909.
Sokolowski, M. B. (2001). Drosophila: genetics meets behaviour. *Nat. Rev. Genet.* **2**, 879-890.
Stocker, R. F. (1994). The organization of the chemosensory system in Drosophila melanogaster: a review. *Cell Tissue Res.* **275**, 3-26.

Journal of Experimental Biology

Stocker, R. F. (2008). Design of the larval chemosensory system. *Adv. Exp. Med. Biol.* **628**, 69-81.
Tissot, M. and Stocker, R. F. (2000). Metamorphosis in Drosophila and other insects: the fate of neurons throughout the stages. *Prog. Neurobiol.* **62**, 89-111.
Tracey, W. D., Jr, Wilson, R. I., Laurent, G. and Benzer, S. (2003). painless, a Drosophila gene essential for nociception. *Cell* **113**, 261-273.
Truman, J. W. (1996). Metamorphosis of the insect nervous system. In *Metamorphosis: Postembryonic Reprogramming of Gene Expression in Amphibian and Insect Cells* (ed. L. I. Gilbert, J. R. Tata and B. G. Atkinson), pp. 283-320. San Diego: Academic Press.
Tully, T. and Quinn, W. G. (1985). Classical conditioning and retention in normal and mutant Drosophila melanogaster. *J. Comp. Physiol. A* **157**, 263-277.
Venken, K. J. T., Simpson, J. H. and Bellen, H. J. (2011). Genetic manipulation of genes and cells in the nervous system of the fruit fly. *Neuron* **72**, 202-230.
von Essen, A. M. H. J., Pauls, D., Thum, A. S. and Sprecher, S. G. (2011). Capacity of visual classical conditioning in Drosophila larvae. *Behav. Neurosci.* **125**, 921-929.
Vosshall, L. B. and Stocker, R. F. (2007). Molecular architecture of smell and taste in Drosophila. *Annu. Rev. Neurosci.* **30**, 505-533.
Zhang, B., Freemann, M. R. and Waddell, S. (2010). *Drosophila Neurobiology: A Laboratory Manual*. New York: Cold Spring Harbor Laboratory Press.
Zwart, M. F., Pulver, S. R., Truman, J. W., Fushiki, A., Fetter, R. D., Cardona, A. and Landgraf, M. (2016). Selective inhibition mediates the sequential recruitment of motor pools. *Neuron* **91**, 615-628.

COMPARISON OF OLFACTORY AND GUSTATORY PREFERENCE BETWEEN STAGE 1 AND STAGE 3 LARVAE

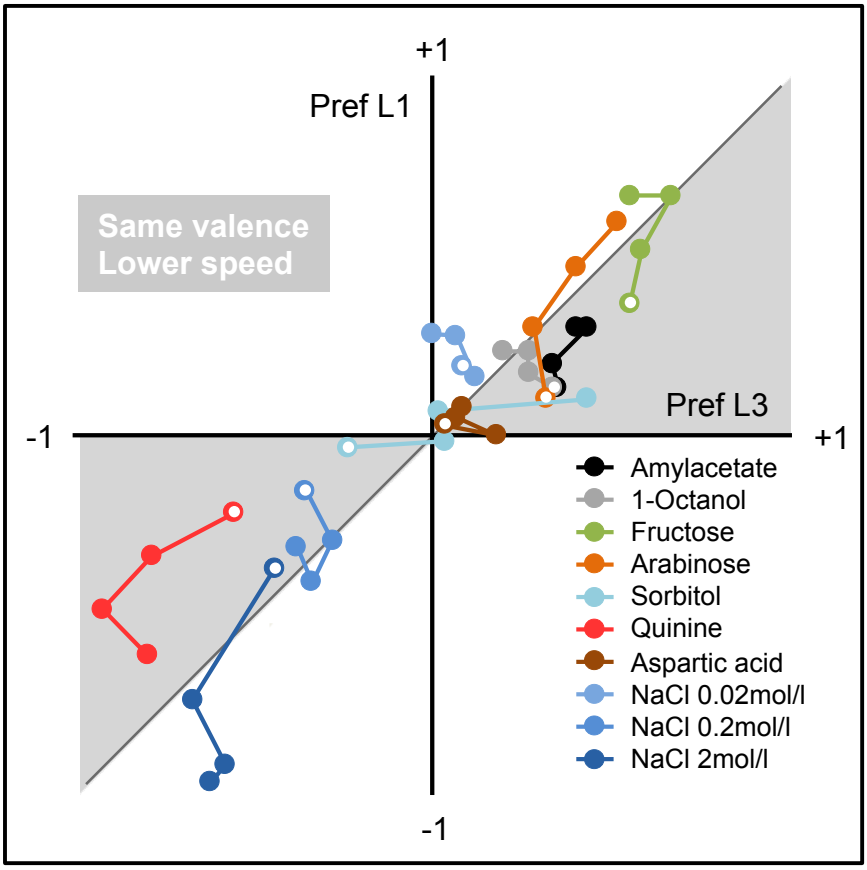

Fig. S1

Fig. S1: ***Comparison of olfactory and gustatory preference between stage 1 and stage 3 larvae***

Plot of the median olfactory and gustatory preference scores of stage 1 larvae (L1) and stage 3 larvae (L3) taken from Fig. 1 and Fig. 2. If both valence and speed were equal between L1 and L3, data would fall onto the diagonal. If valence were qualitatively the same, yet e.g. speed were reduced in L1, preference scores should have the same sign yet be consistently closer to zero in L1 than in L3 such that data points would fall into the grey shaded areas. This is observed for all tested odours and tastants, excepting low-salt and high-salt. In these two exceptional cases, L1 show significantly stronger attraction and stronger avoidance, respectively, than L3. Obviously, these effects cannot be accounted for by the lower speed of locomotion in L1 (see Fig. 7, S4). The white dot represents the respectively first time point of measurement.

FOOD INTAKE

A

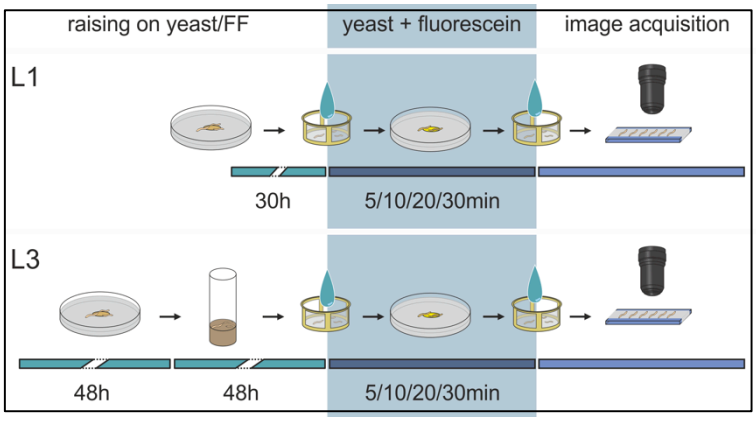

B

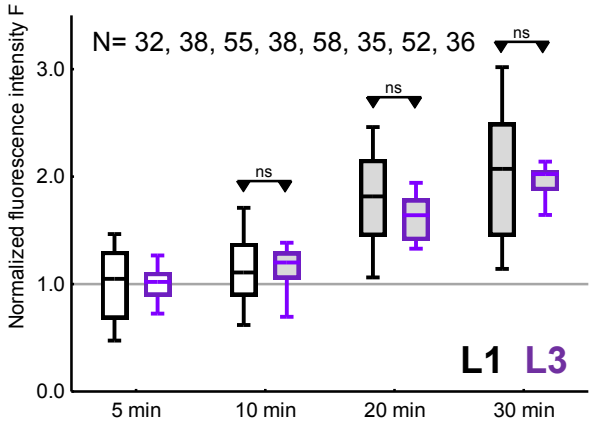

Fig. S2

Fig. S2: *Food intake*

(A) Sketch of the food intake assay. Stage 1 and stage 3 larvae were allowed to feed from yeast paste supplemented with fluorescein (blue shading). After 5, 10, 20, and 30 min fluorescence was measured.

(B) Time course of food intake. Shown is the fluorescence intensity *F* for stage 1 larva (L1, black-line box plots) or stage 3 larvae (L3, magenta-line box plots), separately normalized to fluorescence after 5 min (grey baseline against further increases are judged; therefore data at the 5 min time point are not statistically compared). For both stages a steep increase in food intake is seen between 10 min and 20 min; the time course of food intake appears indistinguishable between L1 and L3.

ns refers to MWU comparisons between groups ($P< 0.05/3$); grey shading of the box plots indicates Bonferroni-corrected within-group significance from zero in OSS tests ($P< 0.05/3$). Data at time point 5 min are not statistically compared, because scores at this time point were defined to be 1, as described in the Materials & Methods section.

Sample sizes are given within the figure.

BURROWING

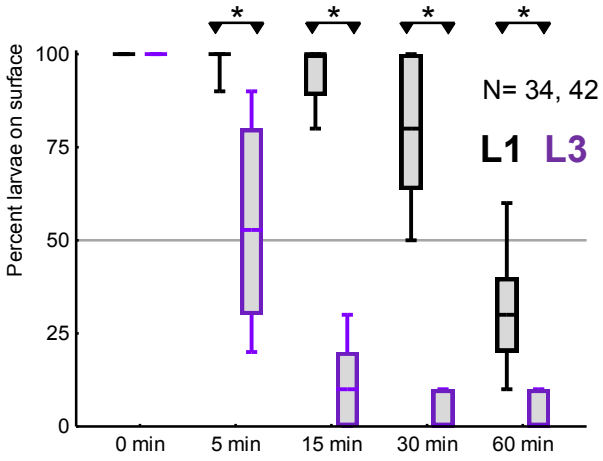

Fig. S3

Fig. S3: *Burrowing*

Groups of 10 larvae (either stage 1 larvae, L1, black-line box plots, or stage 3 larvae, L3, magenta-line box plots) were placed onto a yeast-diet substrate and the percentage of larvae visible on the surface was determined at 0, 5, 15, 30, and 60 min. L1 are significantly slower in burrowing into the substrate than L3.

* refers to Bonferroni-corrected MWU comparisons between L1 and L3 ($P < 0.05/4$). Data at time point 0 min are not statistically compared, because per the experimental procedures all larvae were located on the surface.

Sample sizes are given within the figure.

VIDEO-TRACKING OF THE RESPONSE TO `BUZZ´ MECHANOSENSORY DISTURBANCE

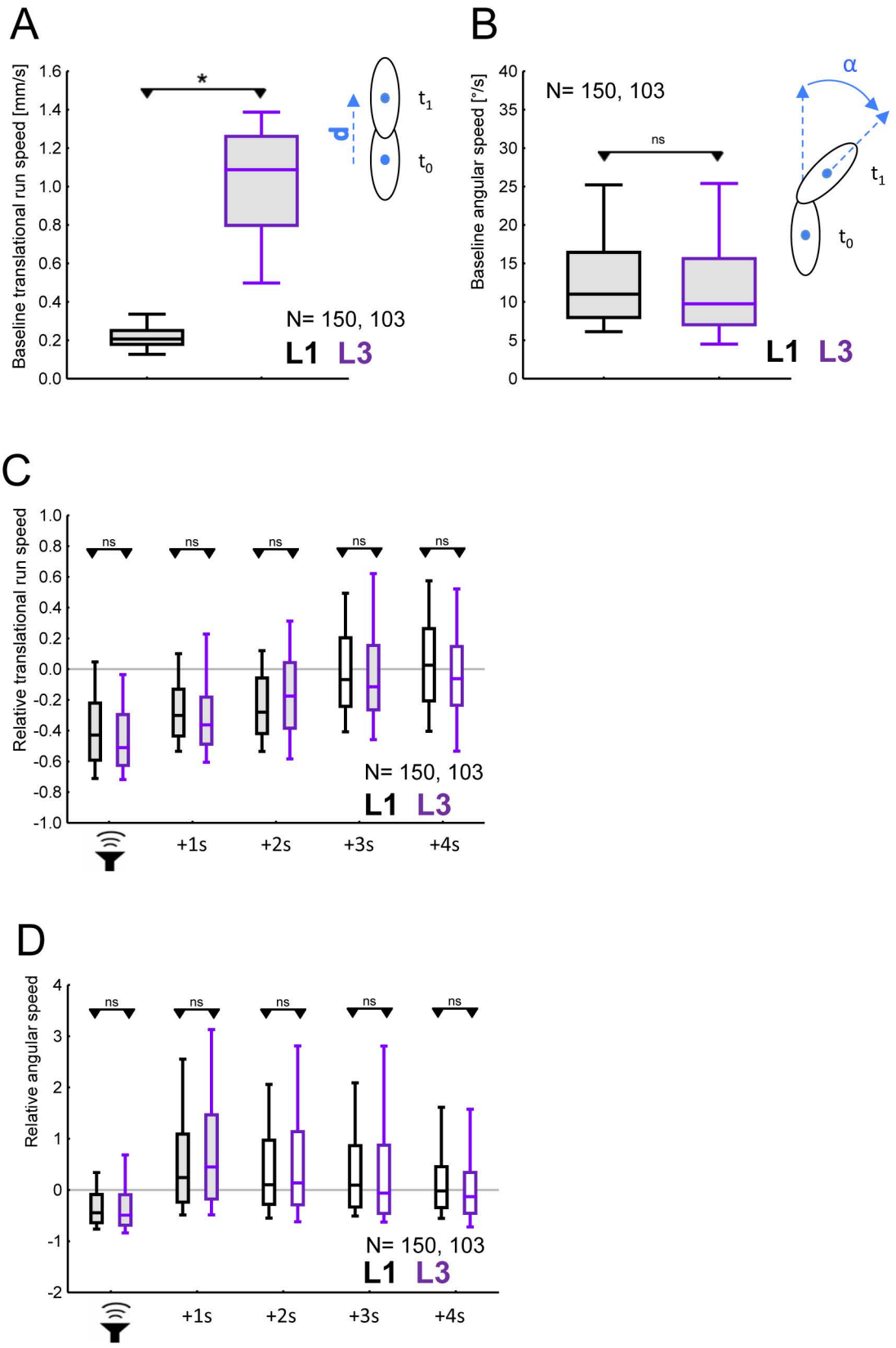

Fig. S4

Fig. S4: ***Video-tracking of the response to a 'Buzz' mechanosensory disturbance***

(A, B) Baseline translational run speed and baseline angular speed. Shown are baseline translational run speed (mm/s) and baseline angular speed (°/s) of stage 1 larvae (L1, black-line box plots) or stage 3 larvae (L3, magenta-line box plots) during a 2-s time window before the Buzz. L1 have about 5-fold lower baseline translational run speed than L3. Baseline angular speed is not different between L1 and L3.

* and ns refer to MWU comparisons between L1 and L3 ($P < \text{or} > 0.05$).

(C, D) Relative translational run speed and relative angular speed during and after the 'Buzz'. (C) Shows run speed, for each individual larva normalized to the 2 s before the 0.2-s/ 100-Hz Buzz mechanical disturbance was delivered. Data are separated in 1-s bins for the 4 s after Buzz onset. (D) Shows the same as in (C), for angular speed. Both L1 and L3 show startle behaviour, in that they hunch and slow down, and then turn.

* and ns refer to Bonferroni-corrected MWU comparisons between L1 and L3 ($P < \text{or} > 0.05/5$); grey shading of the box plots indicates Bonferroni-corrected within-group significance from zero in OSS tests ($P < 0.05/5$).

Sample sizes are given within the figure.

VIDEO-TRACKING OF LIGHT AVOIDANCE

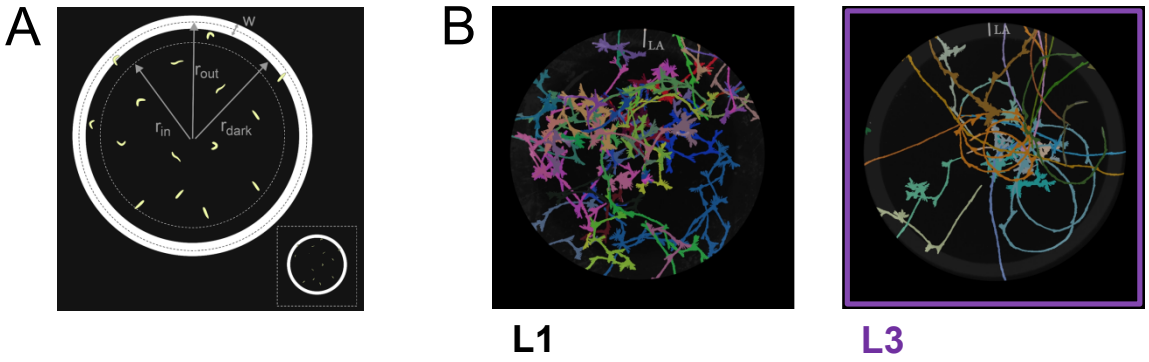

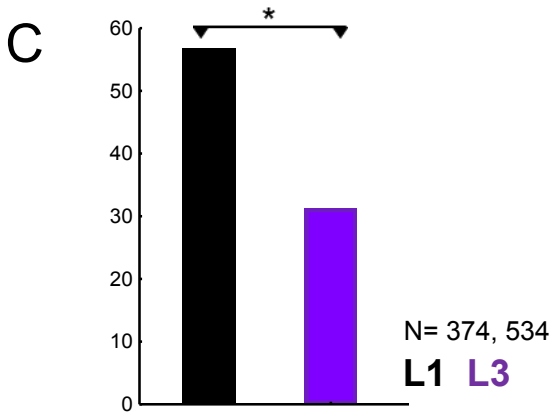

Fig. S5

Fig. S5: ***Video-tracking of light avoidance***

(A) Sketch of the light avoidance setup, consisting of an inner dark area (according to the radius r_{dark}), an annulus of light (of width w), and the indicated dark-light border zone (according to r_{in} and r_{out}). Dimensions were adjusted according to the differences in body length between stage 1 and stage 3 larvae (L1 and L3, respectively) (see Methods section); the inset shows the set-up used for stage 1 larvae for comparison.

(B) Screen-shots of the final frames of Movies 10 and 11 with tracks of stage 1 and stage 3 larvae (L1 and L3, respectively). Dimensions were normalized to body length. The width of the light annulus is indicated (LA).

(C) Percentage of larvae showing avoidance behaviour at the dark-light border zone. This is the case more often for stage 1 than for stage 3 (L1 and L3, respectively), suggesting stage 1 is more light averse than stage 3. * refers to a two-tailed z-test between L1 and L3 ($P< 0.05$) (XLSTAT, Statcon, Witzenhausen, Germany).

Sample sizes are given within the figure.

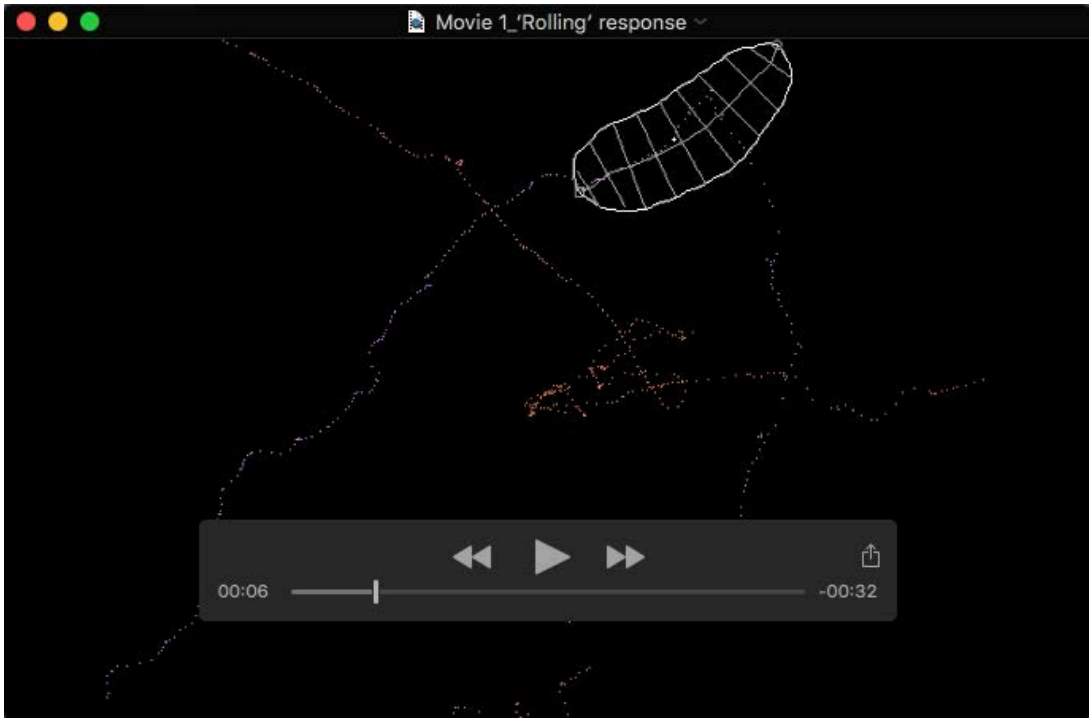

Movie 1: Example of rolling behaviour in response to optogenetic activation of Basin interneurons in individual stage 1 and stage 3 larvae

Tracked rolling behaviour of an individual stage 1 larva (a) and a stage 3 larva (b) expressing Chrimson in the Basin interneurons (R72F11-Gal4 x UAS-Chrimson) upon light stimulation starting at 4 s. Frame rate: 26 frames/s.

Movie 2: Example go-phases of individual stage 1 and stage 3 larvae

Examples of go-phases (125 frames, 12.5 s) of a stage 1 larva (L1, top) and a stage 3 larva (L3, bottom) using the FIM tracking system. Note that the peristaltic pattern in the stage 1 larva is less regular than in stage 3.

Movie 3: Free locomotion of groups of stage 1 and stage 3 larvae

(A) Showing a group of stage 1 larvae moving freely in the 55 mm x 55 mm test arena for 7 min (5-fold time-lapse) recorded with FIM and analysed with FIMTrack (Risse et al. 2013; Risse et al. 2014). Trajectories are blended in after 25 s. The larvae alternate between brief go and reorientation phases; most of the phase transitions lead to changes in bearing > 30° which we defined as turns (Fig. 7G). When compared to stage 3 larvae (Movie 5), the relatively smaller 'exploration range' in stage 1 larvae (Fig. 7H) manifests largely by differences in bending and turning behaviour (Fig. 7F, G), rather than in speed (Fig. 7E).

(B) Likewise showing a group of stage 3 larvae moving freely in the 225 mm x 225 mm test arena for 5.3 min (5-fold time-lapse) recorded with FIM and

analysed with FIMTrack (Risse et al. 2013; Risse et al. 2014). Trajectories are blended in after 15 s. Similar to stage 1 larvae, also stage 3 larvae alternate between go- and reorientation phases, however relatively fewer of the phase transitions lead to changes in bearing > 30° which we defined as turns (Fig. 7G). Together with differences in bending behaviour (Fig. 7F), this results in a larger exploration range in stage 3 than in stage 1 larvae, even when normalized to body length (Fig. 7H).

Movie 4: 'Buzz' response of stage 1 and stage 3 larvae

(A) Showing examples of stage 1 larval behaviour before, during, and after presentation of three consecutive Buzzes (only behaviour in response to the first Buzz was analysed in Figure S4). The white dot in the lower right panel indicates the presentation of the Buzz. Note that the animals startle in response to the Buzz, i.e. hunch and slow down, and then turn.

(B) Likewise showing examples of stage 3 larval behaviour before, during, and after presentation of three consecutive Buzzes (only behaviour in response to the first Buzz was analysed in Figure S4). The white dot in the lower right panel indicates the presentation of the Buzz. Note that the animals startle in response to the Buzz, i.e. hunch and slow down, and then turn.

Journal of Experimental Biology • Supplementary information

Movie 5: Thermotaxis of groups of stage 1 and stage 3 larvae

(A) Showing stage 1 larvae moving in a 55 mm x 55 mm arena as described for Movie 4. Larval behaviour is observed within a linear 0.08 °C/mm heat gradient between 33 °C and 29 °C for 7 min (5-fold time-lapse). Larvae are placed at about 33 °C. Tracks are blended in after 23 s.

(B) Likewise showing stage 3 larvae moving in a 225 mm x 225 mm arena as described for Movie 5. Larval behaviour is observed within a linear 0.08 °C/mm heat gradient between 33 °C and 18 °C for 5 min (5-fold time-lapse). Larvae are placed at about 33°C. Tracks are blended in after 15 s.

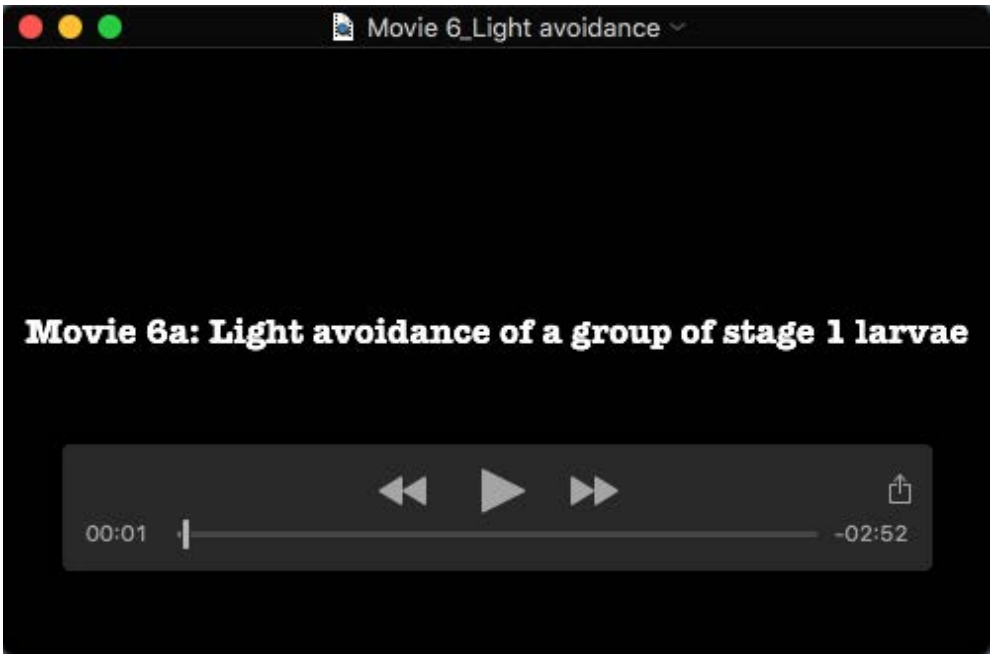

Movie 6: Light avoidance of groups of stage 1 and stage 3 larvae

(A) Showing stage 1 larvae moving in a central dark area surrounded by a light annulus of the indicated width (w) for 7 min (5 fold time-lapse). From 26 s onwards, r_{in} and r_{out} and larval trajectories are blended in (Fig. S5A). The flags are set to define r_{in} and r_{out}. Trajectories are boldened after 73 s. Light avoidance is measured in the dark-light border zone (r_{out} - r_{in}).

(B) Likewise showing stage 3 larvae moving in a central dark area surrounded by a light annulus of the indicated width (w) for 7 min (5 fold time-lapse). From 26 s onwards, r_{in} and r_{out} and larval trajectories are blended in (Fig. S5A). The flags are set to define r_{in} and r_{out}. Trajectories are boldened after 73 s. Light avoidance is measured in the dark-light border zone (r_{out} - r_{in}).

Journal of Experimental Biology • Supplementary information

Table S1

The table presents the data underlying the displayed figures and reported statistics.

Click here to Download Table S1